FEDERAL UNIVERSITY OF RIO GRANDE DO SUL
ENGINEERING SCHOOL
ENERGY ENGINEERING

THERMOENERGETIC PERFORMANCE OF A BUILDING WITH MATERIALS OF PHASE CHANGE UNDER CLIMATE CHANGE PROJECTIONS

per

Lorenzo Olivo Filippini

Monograph presented to the Graduation Committee of the Energy Engineering Course at the School of Engineering of the Federal University of Rio Grande do Sul, as part of the requirements for obtaining a Bachelor's degree in Energy Engineering.

Porto Alegre, April 2023

FEDERAL UNIVERSITY OF RIO GRANDE DO SUL
ENGINEERING SCHOOL
ENERGY ENGINEERING

THERMOENERGETIC PERFORMANCE OF A BUILDING WITH MATERIALS PHASE CHANGE UNDER CLIMATE CHANGE PROJECTIONS

per

Lorenzo Olivo Filippini

THIS MONOGRAPH WAS DEEMED SUITABLE AS PART OF THE REQUIREMENTS FOR OBTAINING THE BACHELOR'S DEGREE IN ENERGY ENGINEERING.
APPROVED IN ITS FINAL FORM BY THE EXAMINING BOARD

Prof. Dr. Thamy Cristina Hayashi
Energy Engineering Course Coordinator

Advisor: Prof. Dr. Letícia Jenisch Rodrigues
Co-supervisor: Prof. Dr. Marcelo Schramm

Examination Board:

Prof. Dr. Letícia Jenisch Rodrigues – DEMEC / UFRGS
Prof. Dr. Marcelo Schramm – Engineering Center / UFPel
Prof. Dr. Cirilo Seppi Bresolin – DEMEC / UFRGS
Prof. Dr. Maurício Carvalho Ayres Torres – FAU / UFRGS

Porto Alegre, April 19, 2023.

FILIPPINI, LO Thermoenergetic Performance of a Building With Phase Change Materials Under Climate Change Projections. 2023. 35 pages. Monograph (Course Completion Work in Energy Engineering) – School of Engineering, Federal University of Rio Grande do Sul, Porto Alegre, 2023.

SUMMARY

The present work investigates the thermal and energy performance of a building with different envelope compositions and its response to future climate scenarios, considering projections of climate changes. Through computer simulations using the EnergyPlus software, the envelope of the building is altered by applying resistive thermal insulation, phase change material or no insulating material and simulated in bioclimatic zones 1 and 8, according to the Brazilian Association of Technical Standards (ABNT); the building, of the light framing type, is built in accordance with normative guidelines from the American Society of Heating, Refrigeration and Air-Conditioning Engineers (ASHRAE). The phase change material used, SP24E, has operating temperatures consistent with the setpoints of the modeled air conditioning system. Using the Climate Change World Weather File Generator (CCWorldWeatherGen) tool, climate change behaviors for the representative years 2050 and 2080 are incorporated into the climate files through the downscaling technique

statistical morphing, considering the A2 (medium-high) emissions scenario from the Intergovernmental Panel on Climate Change (IPCC). The results demonstrate that, in mild climates, such as Curitiba, the phase change material is more efficient than the resistive thermal insulator under climate change scenarios, reducing the annual Energy Use Intensity (EUI) projected for 2050 by 8. 2% and, for 2080, by 10%. For Rio de Janeiro, in climate projections, the envelope with phase change material results in higher EUI, registering 12.1% in 2050 and 20.7% in 2080, more than the envelope with thermal insulators resistive.

KEYWORDS: Phase Change Materials (PCM), Thermal Insulators, Envelope, Energy Efficiency in Buildings, Climate Change, Future Climates.

FILIPPINI, LO Thermoenergetic Performance of a Building with Phase Change Materials Under Climate Change Projections. 2023. 35 pages. Monograph (Work Completion of Graduation in Energy Engineering) – School of Engineering, Federal University of Rio Grande do Sul, Porto Alegre, 2023.

ABTRACT

This paper investigates the thermal and energy performance of a building with different envelope compositions and its response to future climate scenarios, considering climate change projections. Through computer simulations using EnergyPlus, the building envelope is altered by applying resistive thermal insulation, phase change material, or no insulating material at all, and simulated in bioclimatic zones 1 and 8, according to the Brazilian Association of Technical Standards (ABNT); the building, of the light framing type, is built according to American Society of Heating, Refrigeration and Air-Conditioning Engineers (ASHRAE) guidelines. The phase change material used, SP24E, has operating temperatures consistent with the setpoints of the modeled HVAC system. Using the Climate Change World Weather File Generator (CCWorldWeatherGen) tool, climate change behaviors for the representative years 2050 and 2080 are incorporated into the climate files through the statistical downscaling technique morphing, considering the A2 emissions scenario (medium-high) of the Intergovernmental Panel on Climate Change (IPCC). The results show that in mild climates, such as in Curitiba, the phase change material proves to be more efficient than the resistive thermal insulator under climate change scenarios, reducing the annual Energy Use Intensity (EUI) projected for 2050 by 8.2% and, for 2080, by 10%. For Rio de Janeiro, in the climate projections, the envelope with phase change material results in higher EUI, registering 12.1% in 2050 and 20.7% more in 2080 than the envelope with resistive thermal insulators.

KEY WORDS: Phase Change Materials (PCM), Thermal Insulation, Building Envelope, Energy Efficiency in Buildings, Climate Change, Future Climates.

LIST OF FIGURES

LIST OF TABLES

LIST OF FRAMEWORKS

LIST OF ABBREVIATIONS AND ACRONYMS

ABNT	Brazilian Association of Technical Standards
ASHRAE	American Society of Heating, Refrigeration and Air-conditioning Engineers
HVAC	Heating, Ventilation and Air Conditioning
CCWorldWeatherGen	Climate Change World Weather Generator
CondFD	Conduction Finite Difference
COP	Coefficient of Performance
CTF	Conduction Transfer Functions
DONATE	United States Department of Energy
EPE	Energy research company
epw	Energy Plus Weather
HadCM3	Hadley Center Coupled Model version 3
IEA	International Energy Agency
INMET	National Institute of Meteorology
IPCC	Intergovernmental Panel on Climate Change
PACU	Packaged Air-Conditioning Unit
PCM	Phase Change Material
RTU	Rooftop Unit
SWERA	Solar and Wind Energy Resource Assessment
TMY	Typical Meteorological Year
TRY	Typical Reference Year
VAV	Variable Air Volume
WMO	World Meteorological Organization
ZB	Bioclimatic Zone

LIST OF SYMBOLS

	Surface area [m²]
	Monthly heat balance through the internal surface [kWh/m²]
	Specific Heat [W/kgK]
	Thermal capacitance [W/K]
ÿ	Convection heat transfer coefficient [W/m²K]
	Pearson Correlation Coefficient [-]
	Discretization Coefficient [-]
	Slope coefficient of the phase transition process (non-pure materials) [-]
	Thermal Conductivity [W/mK]
	Thermal Diffusivity [m²/s]
ÿ	Nodal distance [m]
EUI	Energy Use Intensity [kWh/m²]
	Thickness [cm]
ÿÿ	Heat flow [W/m²]
ÿÿ	Hourly heat flux through the inner face [W/m²]
	Mass of material [kg]
	Specific mass [kg/m³]
	Fourier number [-]
ÿ	Time step [s]
	Thermal Resistance [m²K/W]
_	Subindex referring to the final state in the phase change process
_	Subindex referring to the initial state in the phase change process
_ +1	Subindex referring to the node adjacent to the modeled node towards the interior
_ ÿ1	Subindex referring to the node adjacent to the node modeled towards the outside
_	Subindex referring to the external node
_	Subindex referring to the internal node
_1	Subindex referring to the node on the external face of the surface

_two	Subindex referring to the node on the inner face of the surface
–	Sub-index referring to the phase change process
–	Subindex referring to interface node to the right of the modeled node
–	Subindex referring to interface node to the left of the modeled node
–	Subindex referring to modeled node
+1	Superindex referring to the new time step
–	Superindex referring to the previous time step
–	Volumetric heat generation rate [W/m³]
	Temperature [°C]
	Hourly Operating Temperature [°C]
	Hourly Average Radiant Temperature [°C]
	Thermal Transmittance [W/m²K]
ÿÿ	Specific enthalpy variation during phase change [kJ/kg]

LIST OF SYMBOLS IN THE MORPHING PROCESS

ÿ	Absolute monthly difference of the climatological variable (shift)
	Monthly partial variation scale factor of the climatological variable (stretch)
0 ÿ	Monthly average of the reference climatological variable
ÿ ÿ ÿ	Monthly average of the future climatological variable
	Number of years considered
	Number of days in each month
two 0 ÿ	Monthly variance of the reference climatological variable
ÿÿ two ÿ	Monthly variance of the future climatological variable
	Future weather hourly variable
0	Hourly reference climate variable

SUMMARY

1. INTRODUCTION

Buildings, together with the civil construction sector, were responsible for around 30% of final energy use and 27% of CO2 emissions worldwide in 2021 (IEA, 2022b). In the national context, for the same year, buildings comprised around 51% of the country's final electricity consumption, according to the Energy Research Company (EPE, 2022). Consumption with air conditioning and ventilation, globally in 2021, corresponded to around 16% of the final use of electrical energy in buildings, which is equivalent to 10% of the total use of electrical energy in the world in that same year (IEA, 2022c).

Given the worsening of climate change and adverse temperature events, the demand for air conditioning systems only tends to grow, and, according to the International Energy Agency (IEA, 2022d), in the next three decades, the use of air conditioning systems Air conditioning will be one of the main drivers of global electricity demand. For the building sector to comply with and contribute to the net zero scenarios planned for 2030 onwards, significant efforts must be implemented throughout the entire production and operational chain. The existential “paradox” of air conditioning systems, which at the same time guarantee comfortable climates and internal conditions, but reject heat for an increasingly hotter atmosphere, denotes the imperative of applying energy efficiency measures and technological harmony in buildings and their environments. systems.

In response to this, the search for passive and active alternatives that guarantee the thermal resilience of the building and ensure thermal comfort over the long term, taking into account future climate changes, must be taken into account from the design of the building. Accordingly, Yüksek and Karadayi (2017) attest that the envelope contributes to around 60% of the energy cost during the life cycle of a building and, also according to the International Energy Agency (IEA, 2022a), the appropriate project incorporating envelope high performance technology becomes the most effective strategy to mitigate the thermal needs of buildings and ensure the comfort of occupants. In this context, the incorporation of thermal energy storage through latent heat in the envelopes through phase change materials (PCM or Phase Change Materials), aiming at energy efficiency and thermal performance, is considered an advanced and promising technology (LIU et al. , 2018).

With this stated, this monograph aims to evaluate the thermal and energetic performance of a building with different proposed envelopes, using phase change materials, under the consideration of future climate change scenarios and their impacts on national climates. To understand the climatic consequences and the responses of the proposed envelopes, energy consumption with the Heating, Ventilation and Air Conditioning (HVAC) system is studied on a monthly scale.
and the heat balance across the surfaces of the north and south facades and roof; Average radiant temperatures, operative temperatures and heat fluxes through the internal faces of surfaces in characteristic thermal zones are evaluated on an hourly scale, during a typical week, in order to study the reasons for the different consumption and heat balance profiles. Emphasizing PCM, it investigates the behavior of the physical state of the material applied to each surface in order to draw relationships with other metrics and understand the reaction of the selected material to climate change.

The building studied represents the typology of a medium office building and has a thermoenergetic model characterized by a single geometry, however, it has construction and HVAC systems in line with the Standards of the American Society of Heating, Refrigeration and Air Conditioning Engineers (ASHRAE) . The models suitable for the different climates in Brazil are simulated using the EnergyPlus software, version 9.2, (DOE, 2022a) in the cities of Curitiba and Rio de Janeiro, respectively, in bioclimatic zones 1 and 8, according to the Brazilian Standards Association Techniques (ABNT).

Originally, the buildings rely on resistive thermal insulators to adapt the thermal parameters of the external walls and roof established by ASHRAE. The work aims to compare the long-term performances of the reference building without any insulating material, with the designed resistive thermal insulator and the same building in which a PCM geometrically replaces the insulator in question. The same PCM is applied in all climatic regions, its operating temperature matches the setpoints of the existing air conditioning system. Projections for climate change are incorporated into the simulations through climate files, using the statistical morphing process and using data from the A2 (medium-high) emissions scenario made available by the

Intergovernmental Panel on Climate Change (IPCC); the process is carried out using the CCWorldWeatherGen tool, version 1.9, developed by Jentsch et al. (2013), from the University of Southampton (2022). Two periods of climate change are constructed for the reference years 2050 and 2080, taking the TMYx type climate file as a basis for changes.

2 BIBLIOGRAPHIC REVIEW

The envelope is the main building system that reacts to local weather conditions. The trends towards intensifying climate change and rising temperatures at a global level, major challenges for humanity in this century, will have a direct impact on the performance of buildings and energy consumption throughout their existence. For Yuan et al. (2022), remodeling the building envelope proves to be a very important strategy from the point of view of several aspects, especially in the long term: energy savings, improvement of internal microclimates, reduction of pollutants in production and technical feasibility economic. Fang et al. (2014) mentions that constructive elements with high thermal performance, which make up the envelope surfaces, guarantee a reduction in energy consumption for air conditioning and improve thermal comfort.

According to work by D'Agostino et al. (2022), the performances of Net Zero Energy Buildings located in different European cities are analyzed for future climates. An increase of between 99 and 380% in the cooling thermal load is estimated, a behavior opposite to that of the heating load, which has an estimated reduction of between 38 and 57%, depending on the typology and location, for the year 2060. The results demonstrate that zero-energy buildings with lower insulation levels are less sensitive to climate change. Accordingly, Baglivo et al. (2022) explain that buildings in hot climates, in southern Italy, within the legal limits for the envelope, will suffer from overheating in the future – the year 2080 – leading to disproportionate consumption with air conditioning; the authors comment that regulatory limits for envelopes have shown trends towards increasing thermal insulation, characterized by low thermal transmittance. Rodrigues and Fernandes (2020) conducted a study in order to evaluate the risks of overheating of residential buildings in the Mediterranean in future climates, projecting ideal values for thermal transmittance in the year 2050. The results demonstrate that the ideal values of thermal transmittance for current climates will not cause buildings to overheat; In some cases, the transmittance of the envelope may even be reduced, as the reduction in heating load compensates for the increase in cooling load. The last two works mentioned made use of the Climate Change World Weather File Generator (CCWorldWeatherGen) tool to incorporate climate projections into simulations.

Among the solutions that can be implemented in the envelope, it is possible to mention the increase in the thermal mass of the surfaces – improving the retention of thermal energy – and the increase in the thermal resistance of the layers of these surfaces – reducing heat transfer by conduction – according to Zilberberg, Trapper and Isaac (2021). Although common construction materials can function spontaneously as thermal energy stores using sensible heat, the use of latent heat is considerably more interesting from the point of view of the energy density of the process (RATHORE et al., 2022); Resistive thermal insulators are capable of significantly reducing heat flow, on the other hand, they have little influence on energy retention (WANG et al. 2022). Within this context, the storage of thermal energy through latent heat through the application of phase change materials becomes an interesting alternative in the construction of envelopes, with the aim of reducing thermal loads from both heating and cooling.

Phase change materials present dynamic behavior, as they can change their physical state at a specific and almost constant operating temperature in the process. Therefore, the passive or active use of PCMs, linked to other strategies, can favor the their application scenarios. Filippini, Sartori and Torres (2021) evaluated the impact of applying PCM on the thermal comfort of a public school with a standardized project in bioclimatic regions 1 and 8 (ABNT, 2005), with Curitiba and Rio de Janeiro as representative cities. Thermal comfort is regulated through natural ventilation, evaluated according to the adaptive thermal comfort of ASHRAE Standard 55, 2017. The authors report that the PCM with a melting temperature of 21°C obtained significant results in improving thermal comfort in both cities, when applied to the external walls and
with a thickness of 5 cm; for the city of Rio de Janeiro, the PCM with a melting temperature of 27°C

also demonstrated positive results when applied to 5 cm thick coverage, reducing hours spent in thermal discomfort.

Phase change materials perform differently in different climates, as demonstrated by Kalbasi and Hassani (2022). The authors applied phase change materials with different melting points to buildings with envelopes compliant with ASHRAE Standard 90.1, according to the association's climate classifications. With the application of PCM, the period of thermal comfort reduced from 54 to 82% of the time among the 10 climates analyzed, highlighting PCM with melting points of 22°C (suitable for 6 zones) and 23°C (suitable for 8 zones). The authors also mention that applying the material close to the interior of the building translates into longer periods of thermal comfort than scenarios with different implementation positions. Carlucci et al. (2021) conclude that the application of PCM significantly reduces the thermal load of cooling environments; In the study carried out, a plasterboard with microencapsulated PCM application and a melting point of 23°C – Alba Balance produced by Saint Gobain – is applied to buildings in different European climates.

Regarding resistive thermal insulators applied in the national context, through the study by Melo et al. (2015) it was concluded that the maximum limits of thermal transmittance of walls given by ASHRAE Standard 90.1, 2013, are not suitable for hot regions such as Brazil, in which energy consumption with air conditioning is dominated by cooling. The authors note that the use of insulating materials can increase the annual thermal load, reducing spontaneous heat exchange from the internal to the external environment during the night. Collaborating with such results, Kalbasi and Afrand (2022) attest that the use of PCM on walls produces better results, in summer, than thermal insulation.

Such behaviors and results mentioned allow the definition of the guiding hypothesis of the present work: in the climate change scenario, characterized by higher temperatures, the use of PCM in the envelope generates better thermal and energy performance results than thermal insulators.

3 THEORETICAL FOUNDATION

Phase change materials are materials capable of changing their physical state at a convenient temperature, being applied in various industry sectors (food, energy, aerospace, automotive, electronics, among others) for storing thermal energy through latent heat, process also known as LHTES, or Latent Heat Thermal Energy Storage.

3.1 Selection criteria and application methods of phase change materials

The use of phase change materials depends mainly on the desired operating temperature, since, during the physical state transition process, the material presents a low temperature variation, transforming the transferred energy into enthalpy variation. In this way, the selection of the material used starts from determining this temperature, according to Suresh, Hotta and Saha (2022).
Other characteristics of PCM must be observed to extract the greatest potential from its implementation, for example, its thermodynamic, chemical, kinetic and economic properties (RATHORE et al., 2016), as summarized by Liu et al. (2018):

- Thermodynamics: adequate phase change temperature, low phase segregation, high latent heat of fusion per unit volume, high specific heat, high thermal conductivity and low volume variation between physical states;
- Chemicals: non-toxic, low flammability, non-explosive, low corrosivity of construction materials, long-term chemical stability, complete melting and solidification cycles;
- Kinetics: high nucleation rate, absence of subcooling, high crystalline growth rate;
- Economical: low cost, commercial availability; It is
- Others: low environmental impact, non-polluting, recyclable, compatibility with the material used in encapsulation.

The effective application of PCM in the context of civil construction can be carried out through different methods, as mentioned by Liu et al. (2018): direct incorporation, immersion, encapsulation and shape stabilization. Among these, encapsulation is the most promising method for buildings, according to the same authors. The form of encapsulation can also be divided according to the scale of the capsule: nanoencapsulated (1 to 1000), microencapsulated (1 to 1000) and macroencapsulated (>1000

), according to Paroutoglou et al. (2019). Techniques involving low capsule scales (< 1000) incorporate the materials directly into the construction elements, changing the thermal properties of the final system. Macroencapsulation, according to Liu et al. (2018), is the most promising application in the context of buildings (for illustrative purposes, see Appendix A for macroencapsulation alternatives).

3.2 Classification of phase change materials

The basic classification of phase change materials depends on the physical states in which the material will operate, these being solid-solid, solid-gas, solid-liquid and liquid-gas (PAROUTOGLOU et al., 2019). In the context of civil construction, the implementation of solid-liquid PCM is aimed at, due to the operating temperature range of a large portion of materials with this behavior.
Figure 3.1 presents a temperature scale and operating enthalpies of different PCMs.

Figure 3.1 - Operating regions of enthalpy and melting temperature of solid-liquid PCM.

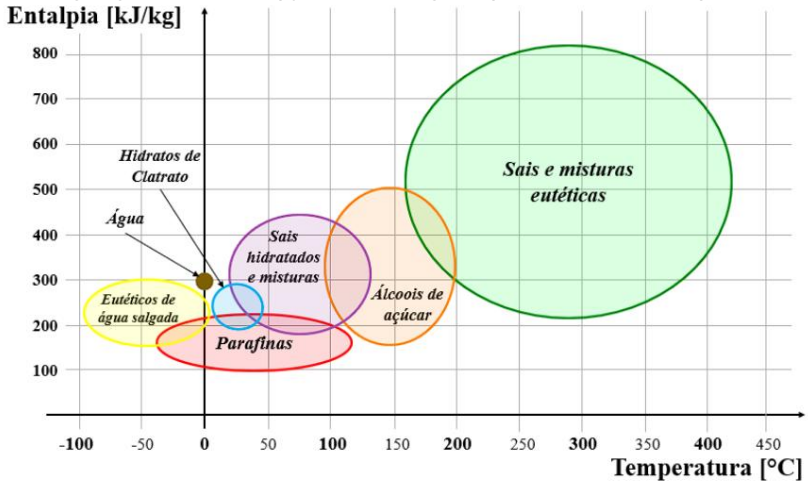

Source: adapted from Al-Yasiri and Szabó (2021).

Within this macrogroup of solid-liquid PCM there are also other classifications, based on the origin and chemical composition of the material. Depending on the classification, these have different properties, which translate into advantages or disadvantages, depending on the application and selection of the material. (see Appendix A). Veerakumar and Sreekumar (2016) briefly describe PCM compositions:

- Organic: carbon-based compounds, generally classified as paraffinic and non-paraffinic paraffinic. •
- Inorganic: generally hydrated or metallic salts. • Eutectics:
- mixtures of two or more PCM to obtain desired operating temperatures. They are also divided based on the melting temperature (high or low) and also by the components of the mixture, being organic, inorganic or organic-inorganic.

3.3 Energy storage by latent heat and thermal hysteresis

Materials can store heat in three different ways: through sensible heat, latent heat and chemical reactions. The process that PCMs perform, regardless of their classification, can be represented by (adapted from AKEIBER et al., 2016):

$$= \ddot{y} \quad ( ) + \quad \ddot{y}\ddot{y} + \ddot{y} \quad ( ) \qquad (3.1)$$

which denotes the energy stored ( ) in the mass of material ( ) within a range of temperatures; ( ) denotes the specific heat of the material as a function of temperature and ÿÿ the specific enthalpy variation of the material in the process. The sub-indices " " refer to the initial and final states, respectively; the subindex " refers to the phase change point. At this temperature value, the physical state of the material effectively changes. Ideally, this change occurs without variations in

temperature, however, in real materials, there may be a variation represented, in the equation, by the coefficient . The integrals refer to sensible heat storage, depending on the mass of the material and its specific heat. The phase change is represented by the enthalpy change of the material (central term of Equation 3.1), that is, the thermal energy received or given up during the phase change comes from the PCM enthalpy conversion.

The cyclic process of phase change in a PCM characterizes its thermal hysteresis phenomenon (shown in Figure 3.2). Zastawna-Rumin, Kisilewicz and Berardi (2020) comment on the occurrence in empirical applications and numerical simulations of PCM, highlighting the importance of the phenomenon for its thermal performance and durability, according to Al-Janabi and Kavgic (2019). Equation 3.1 is applicable to both curves and the area between them establishes the energy stored during the phase change by the material.

Figure 3.2 - Complete thermal hysteresis curve performed by a phase change material.

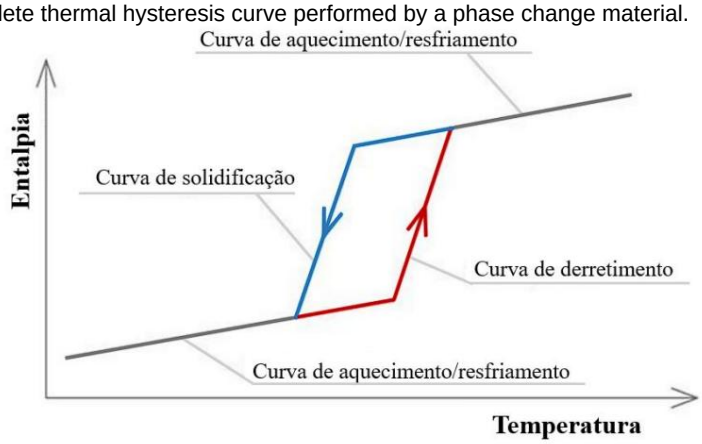

Source: adapted from Zastawna-Rumin, Kisilewicz and Berardi (2020)

3.4 Simulation using EnergyPlus

According to Al-Janabi and Kavgic (2019), the EnergyPlus software is one of the few building simulation tools capable of modeling phase change materials. According to the software's Engineering Reference (DOE, 2019), heat conduction on composite surfaces makes use of CTF (Conduction Transfer Functions) algorithms, developed by the software's precursors, capable of solving the differential equations related to the conduction process. Through the state space method, finite differences are applied to solve the equations, also making use of concepts of thermal circuits of resistance and capacitance. Figure 3.3 presents an interpretation of the algorithm for a system with two nodes.

Figure 3.3 - Construction system with two nodes.

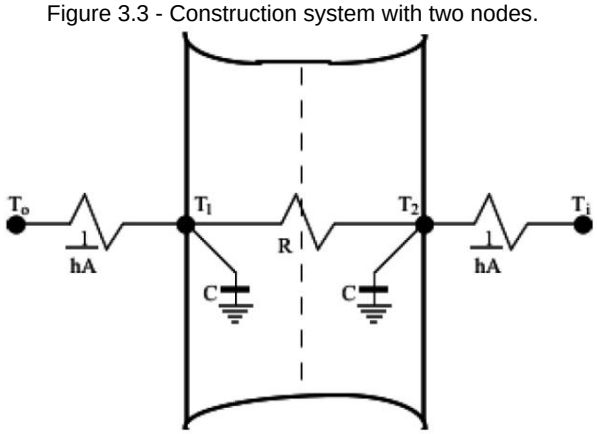

Source: DOE (2019).

Note the representations of thermal resistances ( ) and capacitances ( ) linked to each node and which make up the state space used in the solution, visible through the equations:

$$[\quad] = [\ \ddot{y} \quad \frac{1}{\quad} \quad \frac{1}{\quad} \quad \ddot{y}\ ] + [\ 0 \quad \ddot{y}\ ][\ ] \tag{3.2}$$

$$[\ \ddot{y}\ddot{y}] = [\ddot{y}\ 0\ ][\ 1 \quad] + [\ \ddot{y}\ddot{y}\ 0\ ][\ ] \tag{3.3}$$

In Equations 3.2 and 3.3: represents the node temperature, the surface area, ÿ the convection heat transfer coefficient and " identifies heat flow; the subindices "t" , in this case, refer to the external (outdoor) and internal (indoor) environment. Such a calculation algorithm is the default of the software, and usual building materials can be simulated through it.

The algorithms consider constant thermal properties of the layers and do not produce results on the interior of the surface, therefore, given the change in properties during the phase transition, the use of another more fundamental algorithm, capable of incorporating the dynamic behavior of the PCM, is necessary. To this end, the software, based on user configuration, implements the one-dimensional finite difference algorithm Conduction Finite Difference (CondFD; DOE, 2019). Through it, surface layers are dynamically discretized, based on their thermal properties. In Figure 3.4 this discretization on a complex surface is presented, also illustrating the types of nodes considered by the method.

Figure 3.4 - Spatial discretization of the one-dimensional finite difference method.

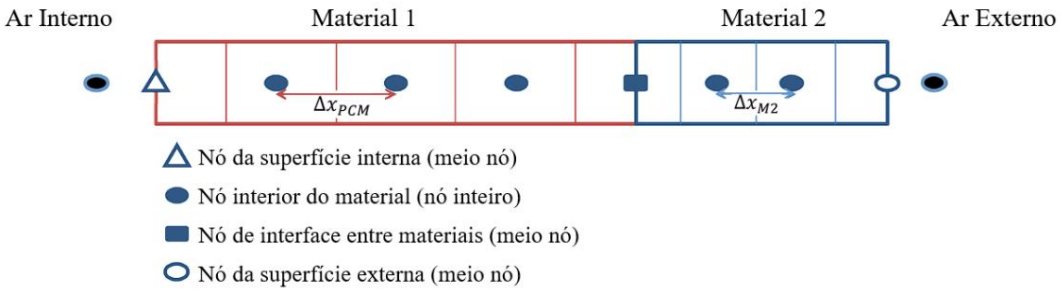

Source: adapted from DOE (2019)

The spatial discretization of each layer of material is carried out by dividing its thickness by a term dependent on the thermal properties of the material and by the time step defined by the user; the term is obtained through:

$$= \ddot{y}\ \ddot{y} \tag{3.4}$$

The integer result of the ratio provides the number of nodes that will be considered by the algorithm to calculate heat transfer; the spacing between the nodes (ÿ) is defined by dividing the thickness of the material by the number of nodes. In Equation 3.4, it represents the thermal diffusivity of the material layer, ÿ the time interval and is the so-called spatial discretization constant, which basically represents the inverse of the numerical Fourier Number (DOE, 2019):

$$= \frac{\ddot{y}}{\ddot{y}2} \tag{3.5}$$

Therefore, the spatial discretization of the method is based on the Von Neumann (or Fourier) stability criterion for an explicit solution method. Such a dimensionless value, according to Bergman et al. (2014), provides a representation of the effectiveness with which the material can conduct and store heat; in this case, ÿ identifies the spacing between nodes and ÿ the time step for each iteration, as in Equation 3.4.

The finite difference method is applied to the one-dimensional heat equation, adapted from Bergman et al. (2014), represented by:

$$=(\quad) + \qquad (3.6)$$

in which the term on the left of the equality represents the stored energy, the first term on the right of the equality the heat flow and represents the volumetric heat generation rate in the evaluated control volume. According to the same authors, the expression denotes that, at any point in the medium where conduction occurs, the net rate of heat transfer in the control volume plus the rate of thermal energy generation must be equal to the rate of change of energy stored in the volume.

As an alternative for solving the finite difference equation, the software presents the possibility of applying two discretization schemes:

$$\ddot{y} \quad \frac{+1}{\ddot{y}} = \frac{1}{\text{two}} \left(\frac{+1 \quad +1}{+1 \quad \ddot{y}} + \frac{+1 \quad +1}{\ddot{y}1 \quad \ddot{y}} + \frac{+1}{\ddot{y}} + \frac{\ddot{y}1}{\ddot{y}} \right) \qquad \ddot{y} \ ) \quad (3.7)$$

$$\ddot{y} \quad \frac{+1}{\ddot{y}} = \left(\frac{+1 \quad +1}{+1 \quad \ddot{y}} + \frac{+1 \quad +1}{\ddot{y}1 \quad \ddot{y}} \right) \qquad (3.8)$$

Equation 3.7 identifies Crank Nicholson's semi-implicit second-order scheme in time and Equation 3.8 the fully implicit first-order scheme in time, both based on the Adams-Moulton solution, according to DOE (2019). In both equations, the temporal and spatial discretizations for each temperature value are explained. The subindexes “W” and “E” refer, respectively, to the nodes to the left (West) and the right (East) of the modeled node, identified by the subindex “ ”; “ÿ1” identifies the adjacent node in the direction towards the interior of the building. The indexes “ ” temporal discretization, where “ ” identifies the previous instant and in the configuration identifies the node adjacent to towards the outside of the building, and, similarly, “ + 1” refers to + 1” the new instant of time, based

Being the implicit solution, the iterative Gauss-Seidel method is used together with a sub-relaxation coefficient to increase numerical stability, thus updating the surface nodal temperatures; The iterative process mentioned is the deepest solver of the CondFD method and is applied to all surfaces. The enthalpy value at each of the nodes is calculated in each iteration. EnergyPlus also performs iterations in an external loop considering the internal energy balance in each of the surface layers, in order to guarantee thermal exchanges arising from long-wave radiation.

To consider the hysteresis phenomenon, the software requires thermodynamic information about the material in both physical states of the process, thus being able to construct the curves that will compose the phenomenon. While the enthalpy of the nodes is calculated in each of the iterations, the specific heat value of the material is also updated, depending on the temperatures and physical states of the node at the beginning and end of the time step.

3.5 Morphing

The basic morphing process, developed by Belcher, Hacker and Powell (2005), changes the original climate variables based on the climate projections of a Global Circulation Model (GCM), however, it respects the meteorological behavior of the base period for modification (baseline). The format of the baseline climate used depends on the format of the data projected in the climate change scenario considered. In the developed method, scenarios are applied that list changes in average monthly climate variables. Thus, the baseline climate behavior

is calculated separately for each month using

$$\ddot{y} \quad 0\ddot{y} = \frac{1}{24} \qquad \ddot{y} \ \ddot{y} \ 0 \qquad (3.9)$$

where the variable denotes the “current” climate record for each month; the climatological reference of this variable in each month is expressed by ÿ ÿ , defined as the average of all years; represents the number of years in the average period and the number of days in each month; 24 expresses the calculation of the hourly average of the variable. This variable ÿ ÿ is used as the current climate reference for direct comparison with climate projections. Depending on the result of this comparison, only one of the operations applies:

$$= \quad _0 + \ddot{y} \tag{3.10}$$

$$= \quad _0 \tag{3.11}$$

$$= \quad _0 + \ddot{y} + (\quad _0 \ddot{y}\ddot{y} \quad _0 \ddot{y}) = \ddot{y} \quad _0 \ddot{y} + \ddot{y} + (1 +)(\ _0 \ddot{y} \ddot{y} \quad _0 \ddot{y}) \tag{3.12}$$

which denote, respectively, the operations of shift, linear stretch and the combination of both, as defined by Belcher, Hacker and Powell (2005). According to the authors' description: the shift operation (3.10) is applied when, in the climate change scenario, there is an absolute variation in the monthly average of variable 0; stretch (3.11) is used when the projected scenario presents partial changes in the mean or monthly variance of the variable, or, when the variable presents a specific and constant behavior during a period, for example, such as solar irradiation, which is zero during the night. The combinatorial shift and stretch operation (3.12) is applied when both the mean and variance of the variable present changes.

In Equations 3.10 and 3.12, ÿ expresses the absolute variation of the monthly average of the variable for the month . As a consequence of the shift process, the monthly variance of the variable is not changed and the calculation of the monthly average of ÿ ÿ becomes

$$\ddot{y} \ddot{y} = \ddot{y} \quad _0 \ddot{y} + \ddot{y} \tag{3.13}$$

In Equations 3.11 and 3.12, the stretch operation identifies a non-integer variation of ÿ ÿ . A scale factor changes the monthly average and the monthly variance of the variable:

$$\ddot{y} \ddot{y} = \ddot{y} \quad _0 \ddot{y} \tag{3.14}$$

$$\ddot{y} \quad ^{two} \ddot{y} = \quad ^{two} \ddot{y} \quad _0 ^{two} \ddot{y} \tag{3.15}$$

When the combined shift and stretch operation is applied, the monthly average of the variable has the behavior given by Equation 3.13, which characterizes the shift process, while the variance ÿ presents the behavior of $^{two}\ddot{y}$ the stretch process given by Equation 3.15.

4 METHODOLOGY

To carry out this work, a generic thermoenergetic model is used. Given the magnitude of the entire national territory, representative cities with different climatic behaviors are defined, in order to evaluate the performance of the building in different application scenarios. Such behaviors are translated through weather files of the Typical Meteorological Year (TMY) type, which are modified using the CCWorldWeatherGen tool. Through this, two new files are created representing future projections incorporating climate change: 2050 and 2080, with TMY as a reference.

The thermoenergetic model is built and made available by the United States Department of Energy (2022b); geometrically it is identical for all climatic zones, however, construction parameters vary according to ASHRAE Standard 90.1 (2019), depending on climatic classifications.
Other systems – ventilation, air conditioning, internal loads – are configured and sized in accordance with this and other association standards. The application of PCM replaces the implemented thermal insulator, respecting its geometric dimensions, thus, the thickness of the PCM is equal to that of the insulator, according to the original thermal parameters of the envelope. Similar to the study by Melo et al. (2015), to

comparison criterion, simulations will be performed where neither insulation nor PCM are applied to the surfaces. All simulations are performed using EnergyPlus and the outputs are analyzed and manipulated using Python scripts, using, in particular, the Pandas library.

4.1 Selection of representative cities

According to ABNT NBR 15220-3 (ABNT, 2005), Brazil is divided into eight bioclimatic zones (ZB). ASHRAE Standard 90.1 (2019) divides Brazil into four climatic regions: 0A (extremely hot humid), 1A (very hot humid), 2A (hot humid) and 3A (warm humid), however, the division of organs is not reciprocal, that is, national climate classifications are not equivalent; for example, the city of Rio de Janeiro, according to ABNT, is located in bioclimatic zone 8 (most extreme), while the American association classifies it in climatic region 1A; the vast majority of cities in climatic region 0A are also in bioclimatic zone 8. As a result, it was decided to prioritize the classification according to ABNT, since it presents greater variability of climates and their characterization for defining guidelines constructive.

In order to evaluate the impact of the envelope in different climatic contexts, cities representing extreme bioclimatic zones 1 and 8, with antagonistic climates, are selected based on the population of each one (IBGE, 2021). Table 4.1 condenses this information.

Table 4.1 - Selected representative cities.

ABNT Bioclimatic Zone (ZB)	ASHRAE Climate Region	Representative city
	3A	Curitiba
1 8	1A	Rio de Janeiro

Source: the Author.

It is worth highlighting, as a limitation of the work, the impossibility of extrapolating the results of the cities to the other locations in their respective bioclimatic zones, since, in zone 8, for example, the vast majority of cities are located in the north and northeast regions of the country, therefore, they present a different solar chart than the city of Rio de Janeiro. January.

4.2 The morphing process and climate files

The morphing process of climate files is carried out using the tool CCWorldWeatherGen, version 1.9. The free tool projects future climate scenarios based on the period from 1961 to 1990 (UNITED KINGDOM, 2022) using data from the global circulation model HadCM3 (Hadley Center Coupled Model version 3), which models atmospheric behavior and oceanic on a global scale; it has a spatial resolution of approximately 300x300 km². Given this low resolution, CCWorldWeatherGen performs a statistical process of dynamic downscaling, and obtains the values of the climate variables for each location by averaging the results of four points on the HadCM3 model's spatial grid closest to the real coordinates of the desired location.

The period considered in the model is in accordance with the World Meteorological Organization (WMO, 2021), which establishes an interval of 30 years as the definition of climate behavior; the organization also maintains the recommendation that the period between 1961 and 1990 be taken as a common reference in studies, projections and monitoring of the climate and its anomalies. Data from the HadCM3 model are made available by the IPCC (2022) and the CCWorldWeatherGen tool considers the IPCC A2 emissions scenario to modify climate files. This scenario projects global economic development with regional growth foci, in a heterogeneous world with a growing population, in which fewer measures in favor of sustainable development are effectively applied, however, it is not the worst scenario in terms of emissions (medium- high). CCWorldWeatherGen transforms an .epw file (EnergyPlus Weather) based on the desired extrapolation for the representative years of 2020, 2050 and 2080, according to the projections obtained by the HadCM3 model, each characterizing a defined climate period of 30 years: 2010 to 2039, 2040 to 2069 and 2070 to 2099, respectively.

Regarding climate data for building simulations in the selected cities, Scheller et al. (2015) carried out a study comparing three types of existing climate files for Brazilian cities: TRY (Test Reference Year), SWERA (Solar and Wind Energy Resource Assessment) and

INMET (National Institute of Meteorology). In the aforementioned work, several meteorological variables from the archives were evaluated. Through this, it was possible to identify that the INMET files had data acquisition failures in some periods, linked to possible problems in the automatic sensors used. Regarding SWERA data, few Brazilian cities have climate files of this type. Therefore, the use of TRY files becomes necessary; files of this type consider a real year within a 10-year period, treating it as a reference year, without temperature extremes. However, according to Crawley and Lawrie (2015), TRY files do not present complete information about solar radiation data, information that was supplied through a new type of file, the Typical Meteorological Year or TMY. This, in addition to having more information than TRY, works with meteorological data from a longer interval, building a fictitious typical year, with months from different years within a period of 15 years or more analyzed. The authors discourage the use of TRY files and recommend using TMY.

Given the considerations and recommendations of Crawley and Lawrie (2015) and the World Meteorological Organization (WMO, 2021), one should opt for TMY type files from older periods or a larger sample of years, to ensure the reliability of the process. of morphing with the projection of realistic weather behaviors. In this sense, we chose to use the TMYx files, which construct typical meteorological years based on the entire existing collection period, made available by
Brazilian Building Labeling Program (2020). The original climate files are presented in Table 4.2, together with the data sampling period.

Table 4.2 - Base climate files for each selected city.

City	Climate file	Period
Curitiba	BRA_PR_Curitiba-Pena.Intl.AP.838400_TMYx	1961-2017
Rio de Janeiro	BRA_RJ_Rio.de.Janeiro-Santos.Dumont.AP.837550_TMYx	1973-2017

Source: the Author.

However, it is important to highlight that the original climate files represent a typical meteorological year within the period described in Table 4.2, considering all years in the sample.
From the beginning of measurements until today, climate change has been part of climate behavior, given that the typical meteorological year encompasses a range of years with this type of behavior, ie, the most recent ones (see Appendix C), and therefore , tends to incorporate the climatological profile with the effects of climate change. Thus, as Jentsch et al. attest. (2013), developers of the tool, and Belcher, Hacker and Powell (2005), developers of the method, it is possible to expect a slight overestimation of the effects of climate change when applying the morphing methodology based on more recent climate files, since the technique maintains the behavior of the original data.

4.3 Thermoenergetic model

ASHRAE Standard 90.1 entitled “Energy Standards for Buildings Except Low Rise Residential Buildings” (ASHRAE, 2019), determines the guidelines for the construction and simulation of thermoenergetic reference models, or baseline models, applicable for all climatic regions. The standard defines the thermal parameters of surfaces, minimum efficiency of air conditioning systems, lighting densities and HVAC systems suitable for construction typologies, according to the floor area and their locations. The thermoenergetic model of this study is developed and made available, in its entirety, by the United States Department of Energy (DOE, 2022b), through the Building Energy Codes Program (BECP), which, together with other typologies, are widely used in several studies, being structured in compliance with the aforementioned Standard 90.1. The set of prototypes represents about 75% of the floor area of new buildings in all North American climates.

This monograph chooses to use the average office building model (Figure 4.1),
typology that generally has integrated projects and systems that have a greater focus on the application of thermal comfort and energy efficiency measures, in addition to, due to the building's operating behavior, being subject to greater thermal loads during critical periods. The models used in bioclimatic zones are identical regarding the type of air conditioning systems, internal loads and building operation, with constructive variations and details of the HVAC system, in accordance with ASHRAE Standard 90.1 (2019). The construction system of the building is steel frame, which, depending on the same

standard, requires the use of thermal insulation on the walls. The maximum thermal transmittance value (U factor or just) for the walls and roof of the models, in each climate zone, are listed in Table 4.1. None of the parameters mentioned, with the exception of climatic conditions, are changed between simulations of the same bioclimatic zone.

Figure 4.1 - Geometric model of the typology.

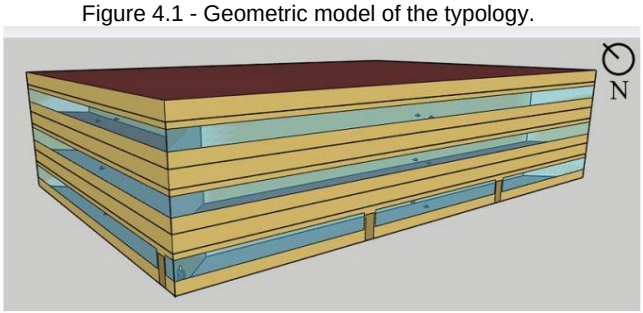

Source: adapted from DOE (2022b).

Table 4.1 - Thermal transmittance of construction surfaces.

Bioclimatic Zone	**[W/m²K]**	**[W/m²K]**
1 (3A)	0.220	0.435
8 (1A)	0.273	0.705

Source: adapted from ASHRAE (2019).

The office building has three floors with 5 thermal zones each, classified as perimeter (1 to 4) or core (5), with the same definitions of internal loads per unit area. Through Figure 4.2 it is possible to visualize the model geometry in greater detail; the percentage of opening area, in all orientations, is 33%. The building's HVAC system is a single-duct, multi-zone variable air volume (VAV) type, where a fan with variable speed blows the mixed air (external and return) and each thermal zone has another fan capable of modulating the airflow. air by *dampers* according to the zone's temperature *setpoints ;* The air cooling and heating system is central, with air reheating units in the thermal zones.

In detail, each of the floors is served by a *self-contained rooftop* unit. *air-conditioner* (or *PACU, Packaged Air-Conditoning Unit)* where the machine has, contained in a single housing, the entire air supply and conditioning system (heating and cooling coils) to serve the floors. The cooling system is through direct vapor expansion, while the heating system is through natural gas, systems with efficiencies of, respectively, 340% (COP) and 81%; each thermal zone has an individual heating system through an electrical resistance at the inflation terminals, with unitary efficiency.

Figure 4.2 - Details of the building geometry and thermal zones.

(a) Numbering and orientation of thermal zones.

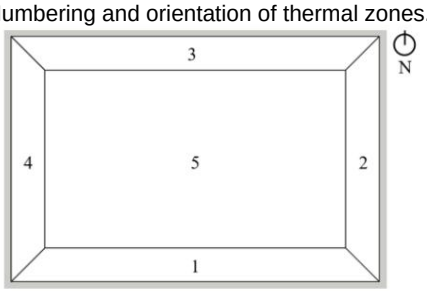

(b) Identification of thermal zones and *plenums.*

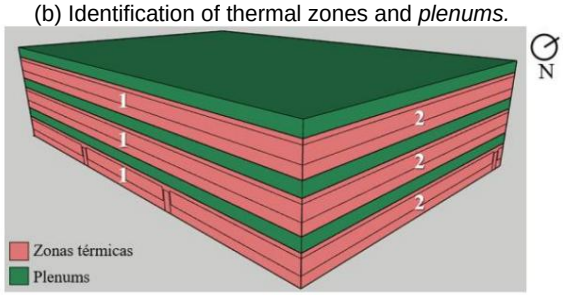

Source: adapted from DOE (2022b).

Between the floors there are return *plenums* for the air conditioning systems that serve each of the respective floors and where, in practice, the ducts and fan boxes for each thermal zone are housed; return air from all areas of the floor is blown into the space. In climate region 3A

(ZB1, Curitiba) the air supply system on each floor has an economizer cycle (see Appendix B), the activation of which depends on the difference in enthalpy between the external air and the return air: if the enthalpy of the external air is greater than that of the return air, the external air flow rate is fixed at a minimum value, otherwise, the *dampers* modulate the air flow rates in order to reach the temperature *setpoint ;* This way, less energy is required to condition the supplied air.

4.4 Phase change material selection and simulation setup

The thermoenergetic model used has heating and cooling *setpoint* values of 21 and 24°C, respectively, which represent temperatures commonly used for activating HVAC systems. The selection of the phase change material, since its implementation aims to reduce energy consumption with air conditioning systems, aims, in short, to guide the temperature of the physical state change according to the operating limits of the air system. conditioning.

For this logic and taking as a reference the selected materials and results in some of the previously described works, we chose to use the SP24E inorganic PCM, produced by RubiTherm (2022b). The manufacturer mentions that, for application in buildings, inorganic materials are generally preferred (RUBITHERM, 2022a). The PCM in question presents favorable characteristics for its selection: stable performance during phase change cycles, high latent heat per unit volume,

limited subcooling, low flammability; It is non-toxic and capable of being macroencapsulated.

The selected PCM is modeled, in *EnergyPlus,* using The class *MaterialProperty:PhaseChangeHisteresys,* capable of modeling the cyclic behavior of the latent phase of materials; the class requests properties of both physical states (see Appendix D). To do so, it is necessary to use the CondFD finite difference algorithm. In agreement with Al-Janabi and Kavgic (2019), due to its robustness and stability, the fully implicit scheme is used, such as the *TARP* algorithms for internal convective exchanges and the *DOE-2* for external convective exchanges. As discretization parameters, the results of Tabares-Velasco, Christensen and Bianchi (2012) were adopted, which validated the values of 0.3 for the discretization constant and 60 time steps per hour, the maximum allowed by EnergyPlus . Such algorithms and configurations are not necessary for simulating envelopes without PCM, but are maintained in favor of standardizing the numerical methodology between simulations. Tolerances for numerical convergences were kept as the *software default values.*

The thickness of the PCM used on each surface is equivalent to the thickness of the insulation applied in each of the respective construction systems, since the aim is to geometrically replace one with the other. According to the models developed by DOE (2022b), the thermal resistances ( ) of the insulators used in each model are visible in Table 4.2; It should be noted that, in thermoenergetic models, insulators are represented only through their thermal resistance values

equivalent, without the definition of a physical material, that is, without thermal mass.

Also according to DOE (2022c), the main thermal insulators used in civil construction are cellulose, glass fiber and mineral fiber, which have a similar thermal conductivity ( ) and can be approximated by 0.04 / (POPESCU, 2017). The theoretical thickness of the insulating material ( ) is given by multiplying the thermal resistance ( ) and the thermal conductivity of that material. This thickness is also the thickness of the PCM that will replace the insulator. Table 4.2 illustrates integer values –

given the need for discreet encapsulation – of the thickness of the PCM applied to each surface according to its climate zone; to illustrate envelope constructions, see Appendix E.

Table 4.2 - Thermal resistance used in each model and material thickness.

Bioclimatic Zone	**External Wall Coverage**			
	[m²K/W]	**[cm]**	**[m²K/W]**	**[cm]**
1 (3A)	4,319	17	1.903	8
8 (1A)	3,472	14	1.037	4

Source: the Author.

5 SIMULATION AND ANALYSIS OF RESULTS

A total of 18 simulations were carried out: 9 simulations for each bioclimatic zone, divided into simulations varying the composition of the envelope (resistive thermal insulation, temperature change material),

phase and no material) for each of the climate files (original TMYx, 2050 projection and 2080 projection). The *morphing* process was performed using the CCWorldWeatherGen tool , generating climate files for the representative years 2050 and 2080 from TMYx. The average duration of simulations using *EnergyPlus* with thermal insulation or no material was approximately 30 to 35 minutes, while when the phase change material was applied, the average simulation time increased to approximately 40 to 45 minutes; the simulations were carried out using an i5-8250U processor and 8 GB of DDR4 RAM.

Metrics for the entire building and some representative thermal zones are evaluated. The thermal zones and spaces selected for analysis are: zone 1 (south facade) and zone 3 (north facade), on the intermediate floor, both occupied and air-conditioned, and the plenum on the *roof* . To evaluate the impact of the envelope and the orientation of the facades, the monthly heat balance is presented for each of the simulated climate behaviors: it expresses the sum of the heat flow by hourly conduction on the inner surface of the surface. The metric results in a net heat gain or loss during the hours of building operation and HVAC system operation. The hourly data of mean radiant temperature, operating temperature and heat flux through the envelope are worked during typical weeks defined by the TMYx climate files (weeks with mean temperatures closest to the mean for each season). We chose to use the average radiant temperature to evaluate thermal zones 1 and 3, unlike the operative temperature, as the environments are conditioned, therefore, the average air temperature approaches the setpoint and, therefore, not illustrating in *a* way the direct impact of the envelope is desired; in parallel, the operating temperature of the *plenum* is investigated, as this environment only has opaque surfaces and is not conditioned, but receives return air from the thermal zones.

Emphasizing phase change materials, the characteristic and predominant clockwise behavior of PCM on the evaluated surface is illustrated. To obtain this information, the representative value of each of the nodes generated by *EnergyPlus* itself is used , which comprises a real number between -2 (liquid) and 2 (solid). From the Mean Value Theorem, a representative numerical value is extracted from the integration of Simpson's Rule; the predominant value is the mode of the nodal results.

In relation to the building, the behaviors of the total monthly energy consumption of the HVAC system are extracted – electrical and thermal, in thermal resistances or direct expansion and gas heater, respectively – already defined in the model, divided by the conditioned floor area, metric represented by *Energy Use Intensity* (EUI) or Energy Use Intensity, with the aim of incorporating the partial load profile that air conditioning equipment can present and studying the impact of the envelope on the typology in question. Table 5.1 summarizes the results of annual Energy Use Intensity with the air conditioning systems for each of the envelopes in the different simulated climate scenarios. The acronyms “NEM”, “ISO” and “PCM” represent the envelopes no material, resistive thermal insulator and phase change material, respectively.

Table 5.1 - Annual Energy Use Intensity (EUI).

Curitiba, PR – Bioclimatic Zone 1/Climatic Region 3A		
Climate	**NEM [kWh/m²]**	**ISO [kWh/m²]**	**PCM [kWh/m²]**
TMYx	37.17	21.17	20.35
Projection 2050	40.49	29.15	26.76
Projection 2080	48.99	35.93	32.34

Rio de Janeiro, RJ – Bioclimatic Zone 8/Climatic Region 1A		
Climate	**NEM [kWh/m²]**	**ISO [kWh/m²]**	**PCM [kWh/m²]**
TMYx	52.38	41.27	38.15
2050 Projection	69.23	50.86	57.03
2080 Projection	80.57	58.38	70.48

Source: the Author.

The results demonstrate lower EUI values for the PCM envelope compared to the others in bioclimatic zone 1 in all simulated climates; for bioclimatic zone 8, the envelope with phase change material presents the lowest EUI value for the typical meteorological year, however, it exhibits superior results to the envelope with resistive thermal insulator in simulations using

climate projections; the envelope without insulating material, that is, with the highest thermal transmittance, presents the highest EUI values in all simulations.

5.1 Results for bioclimatic zone 1/3A (Curitiba, PR)

Through Figure 5.1, it is possible to observe the monthly behavior of the Intensity of Energy Use with the HVAC systems for the city of Curitiba; Considering the typical meteorological year, it is necessary to use heating, especially in the case of the envelope without any material.

Figure 5.1 - Monthly Energy Use Intensity with HVAC systems in Curitiba, PR (ZB1/3A).

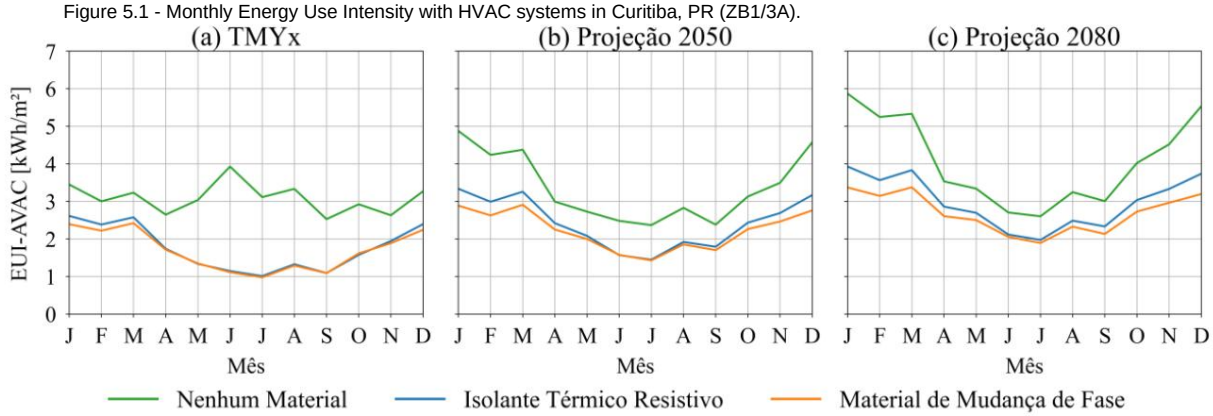

Source: the Author.

Highlighting it in Figure 5.1 (a), consumption in the winter months exceeds consumption in the summer months. This can be justified by the use of the heating system through individual thermal resistances located in the insufflation of the thermal zones. Such equipment has unitary efficiency, which makes it less efficient than the direct expansion system, used to cool environments.
However, the gas central heating system is also required at times during the winter, increasing energy consumption. In comparison with other envelopes, the application of PCM results in an annual EUI that is approximately 82.5% lower during the typical year, and, on average, 51.4% in future climates; the envelope with thermal insulation, in turn, presents an annual EUI during the simulation with a TMYx of 75.4% lower than the envelope without material, and the average of future climates is 37.6% lower. When comparing these composite envelopes with each other, the application of phase change material produces lower annual values: around 3.9% lower in the typical year, 8.2% in 2050 and 10% in 2080.

Due to the increase in temperatures depending on climate projections, there is a change in the behavior of energy consumption during the winter period in the case of buildings without insulating material in the envelope; In both simulated projections, the winter months have the lowest EUI value in the year, that is, the thermal demand for heating is “converted” into thermal demand for cooling. Regarding simulations in which the envelope has either thermal insulation or phase change material, the monthly energy consumption profile is similar and very close throughout the year for the TMYx climate. The “detachment” of consumption curves is notable in the months outside the autumn and winter period in projections of future climates, with a difference of almost 1 kWh/m² in 2080.

5.1.1 North facade (thermal zone 3)

Figure 5.2 illustrates the heat balance on the inner face of the surface ( ), denoting monthly heat gains by the thermal zone when the balance is positive and heat losses by the zone when the balance is negative; the balance represents the sum of the hourly heat fluxes on the internal face of the facade during the building's occupation. It is observed that, for all simulations, the heat balance on the surface with the phase change material is always negative, denoting the removal of heat from the thermal zone during its operation, which reduces the cooling load; This occurs due to the coincidence of the air temperature in the zone with the phase change temperature of the material. During the winter months, especially in Figure 5.2 (a), energy consumption for this envelope decreases, which does not mean that there is a demand for heating, but rather that the thermal zone, through solar gains and loads internal, together with thermal insulation, manages to maintain comfortable levels of

temperature passively. In this sense, the temperature of the internal face can remain close to the solidification temperature of the material, while its core and, mainly, the external face of the facade have lower temperatures, which reduces the rate of heat transfer through this surface.

Figure 5.2 - Monthly heat balance across the north facade in Curitiba, PR (ZB1/3A).

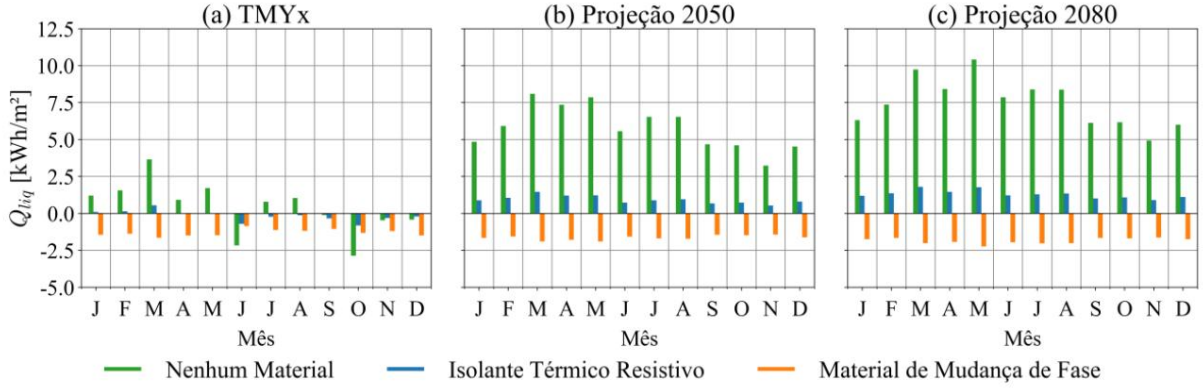

Source: the Author.

The envelope without any material does not show characteristic behavior during the typical meteorological year, having one of the lowest values for the heat balance in the month of June (-2.15 kWh/m²), the month with the highest EUI, of 3.93 kWh/m²; the month of October, outside the intense cold season, during the spring period, presents the lowest value for the heat balance (-2.86 kWh/m²), and, consequently, one of the highest EUI recorded for this envelope (2.95 kWh/m²). The absence of insulating material causes intense heat gains in climate projection simulations, frequently exceeding 5 kWh/m² and 7.5 kWh/m² monthly, reaching maximums of 8.10 kWh/m² in March 2050 and 10.42 kWh/m² in May 2080, due to the intensification of direct solar irradiation during this period. The application of the resistive thermal insulator guarantees the maintenance of low levels of heat gains and losses, as observed in all simulations.

Figure 5.3 - Hourly curves of average radiant temperature in thermal zone 3 and heat flow by conduction on the internal face of the north facade during the typical winter week in Curitiba, PR (ZB1/3A).

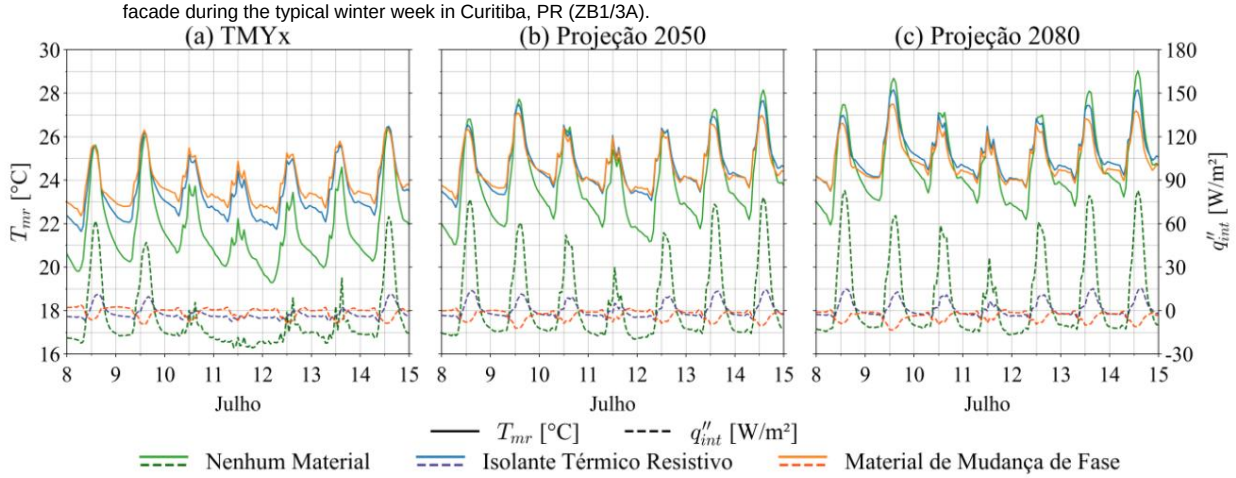

Source: the Author.

The hourly curves of mean radiant temperature ( ) and heat flux by conduction on the inner face of the envelope surface ( ) for thermal zone 3 are expressed in Figure 5.3; the positive direction of heat flow indicates a flow from the outside to the inside of the thermal zone. For Curitiba, we chose to study the profile of the variables in the typical winter week, defined between the 8th and 15th of July, according to the TMYx climate file.

Simulations with phase change material in the envelope, for the typical meteorological year, result in mean radiant temperatures higher than other envelopes, especially among the

busy periods on weekdays, with a weekly average of 24.06°C. During the typical week (Figure 5.3 (a)), at night, unlike wraps with thermal insulation and no material, the conductive heat flow in the wrap with PCM is positive or very close to zero, contrasting with other applications, in which the flow of heat is negative. In this sense, thermal zone 3 loses heat at a lower rate or even receives heat in this interval of hours through the external wall; This passive behavior is complemented by the removal of heat by the PCM during the day, reducing the temperature range. Thus, when the building returns to operation, the following day, the thermal zone presents a higher average radiant temperature, and, consequently, its thermal heating load decreases, especially at the beginning of occupancy. The material stores heat from the thermal zone during the day and is able to release it at night; the average radiant temperature is 24.85°C in the 2050 projection and 25.14°C for 2080, during occupancy hours.

For the climate projections of 2050 and 2080 (Figure 5.3 (b) and (c)), the temperatures of the thermal zone in the simulations with thermal insulator and with PCM become practically identical, with few variations throughout the week, contributing to the similar results for EUI visible in Figure 5.1 (b) in the months of June and July; under the respective climatic conditions, the weekly average radiant temperature is 24.98 and 25.46°C for the insulating envelope. It is interesting to highlight the greater incidence of direct solar radiation during winter, which is translated by the high heat flux in the case without any material in the envelope; in an antagonistic way, the reduction in external temperatures during the night produces temperature gradients of almost 6°C for this envelope, which becomes much more susceptible and sensitive to changes in the weather and local climate, presenting averages of 22. 09°C in the typical year and 24.32 and 25.20°C in the respective future climates, which corroborates the change in the EUI pattern presented by the building with this envelope.

Figure 5.4 - Hourly behavior of the physical state of the PCM applied to the north façade during a typical winter week in Curitiba, PR (ZB1/3A).

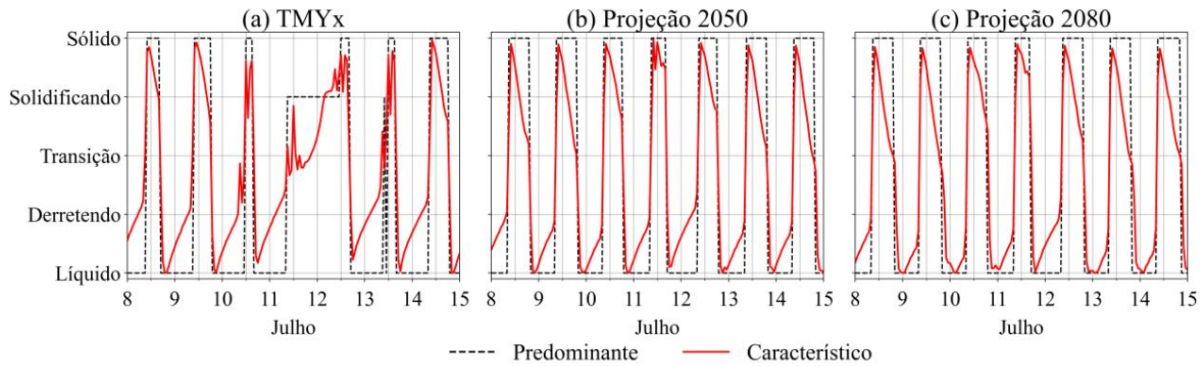

Source: the Author.

The behavior of the heat balance across the facade is complemented by the analysis of the characteristic physical state of the phase change material, through Figure 5.4. In Curitiba, we chose to evaluate the material during the typical winter week, defined by the TMYx file as being between the 8th and 15th of July. When observing all the curves, the cyclical behavior of the physical state is notable, explaining the completeness of the thermal hysteresis process by the PCM on this surface daily: during the beginning of the day, the material solidifies, releasing heat to the surroundings; over time, the material spontaneously removes heat from its surroundings, melting; The PCM's thermal hysteresis cycle occurs within the air conditioning system's *setpoint* range , therefore, exothermic and endothermic processes regulate the temperature of the internal face to levels consistent with the system.

5.1.2 South facade (thermal zone 1)

When looking at Figure 5.5, as in thermal zone 3, for the typical meteorological year (Figure 5.5 (a)) and for the projection for 2050 (b), the thermal zone loses heat intensely, with the minimum in June of the TMY, approximately -6 kWh/m²; In the same way as in thermal zone 3, heat loss through the wall – in cases with PCM – decreases in the winter months, denoting the reduction in demand for spontaneous cooling of the thermal zone.

Figure 5.5 - Monthly heat balance through the south facade in Curitiba, PR (ZB1/3A).

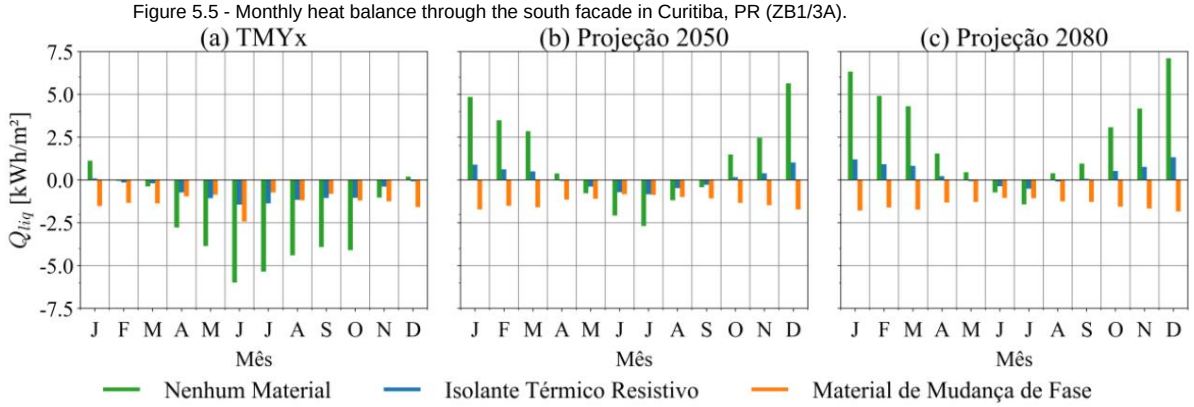

Source: the Author.

Due to heat loss through the envelope on the south facade when no material is applied, the heating load overlaps the cooling load, justifying the longer EUI period for this application; annual heat losses, during the typical meteorological year, reach almost -49 kWh/m². The envelopes with phase change material and thermal insulation, during winter, present similar EUI and heat balance, especially on the south-facing facade. Outside this period, with emphasis on simulated climate projections, the PCM envelope has a better capacity to remove heat from the thermal zone, reducing the cooling load – annually, the PCM facade presents average heat losses of -16.45 kWh /m², while the thermal insulator is -7.28 kWh/m², around 56% lower. The impact of the absence of solar radiation is easily observed through the monthly heat losses through the facade without insulating material.

Figure 5.6 - Hourly curves of average radiant temperature in thermal zone 1 and heat flow by conduction on the internal face of the south facade during a typical winter week in Curitiba, PR (ZB1/3A).

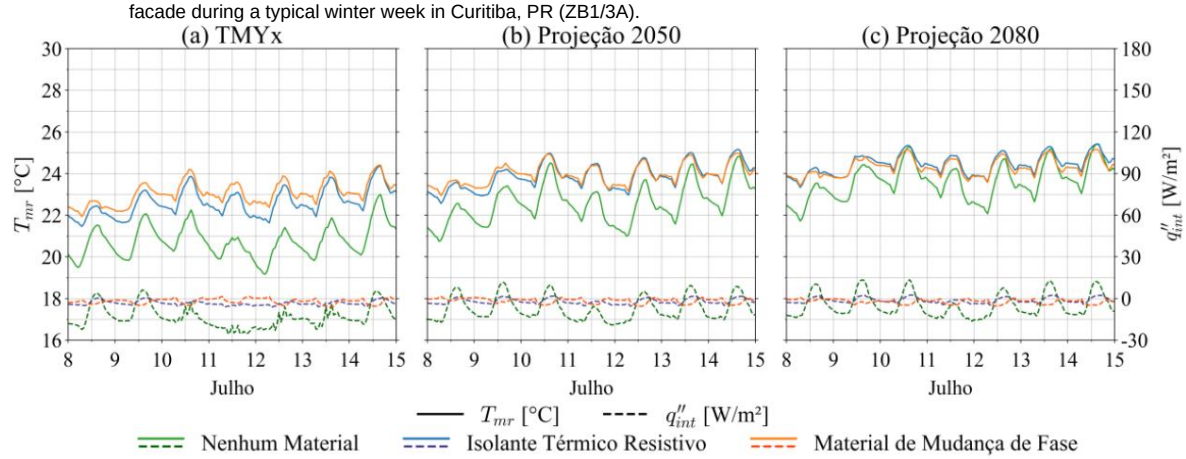

Source: the Author.

In Figure 5.6, as occurs for the north facade, during the typical meteorological year (a) and for the projection for 2050 (b), the conductive heat flux for the PCM envelope remains negative, thus, the area loses heat to the wall with the material. For the simulation using TMY, the average radiant temperature of thermal zone 1 – with PCM in the building envelope – is higher, during all hours when compared to the other cases, reaching 23.23°C weekly average during occupancy.

Similar to thermal zone 3, the heat flux on the inner face of the envelope is positive or null during most of the night hours of the week, especially in Figure 5.6 (a). Such passive heating, due to the storage of thermal energy by the PCM, guarantees lower mean radiant temperature gradients. For this thermal zone, the PCM is capable of maintaining the average radiant temperature during the week between 23 and 24.5°C considering all simulated climates; the envelope without insulating material does not

presents average above 24°C in none of the simulations, during busy hours, with the exception 2080, which registers the highest among the envelopes, equal to 24.57°C.

Regarding the physical state of the material, shown in Figure 5.7, for the climate described by the TMYx file (Figure 5.7 (a)), the predominance of the solid or partially solid state can be noted during much of the typical winter week, maintaining a intermediate state for the period. This can be justified by the low heat fluxes during this interval, given the low external temperature and the proximity of the internal temperature to the PCM operating point. In this sense, the core of the material functions as a barrier for heat transfer between the external environment and the internal environment during phase change; When considering climate changes in the simulations, the PCM presents more evident daily phase change cycles, especially exposed Figure 5.7 (c), indicating that the performance of the material improves in future climates for this facade, which also corroborates the intensification of heat removal from the thermal zone in these simulations.

Figure 5.7 - Hourly behavior of the physical state of the PCM applied to the south facade during a typical winter week in Curitiba, PR (ZB1/3A).

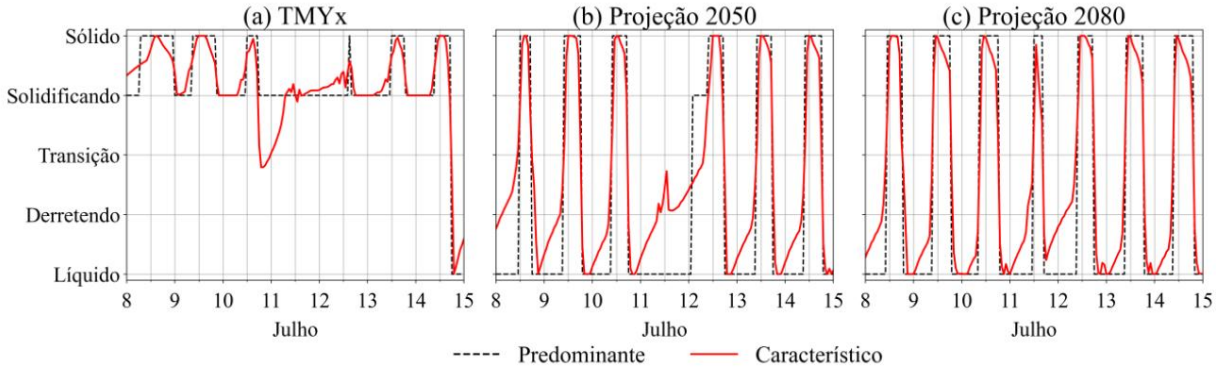

Source: the Author.

5.1.3 Coverage *(plenum)*

Due to the thickness of the insulating material on the roof (17 cm), both resistive and phase change material, the heat flow is extremely low, resulting in monthly heat balances close to zero in these roofs, as can be seen in Figure 5.8.

Figure 5.8 - Monthly heat balance through the roof in Curitiba, PR (ZB1/3A).

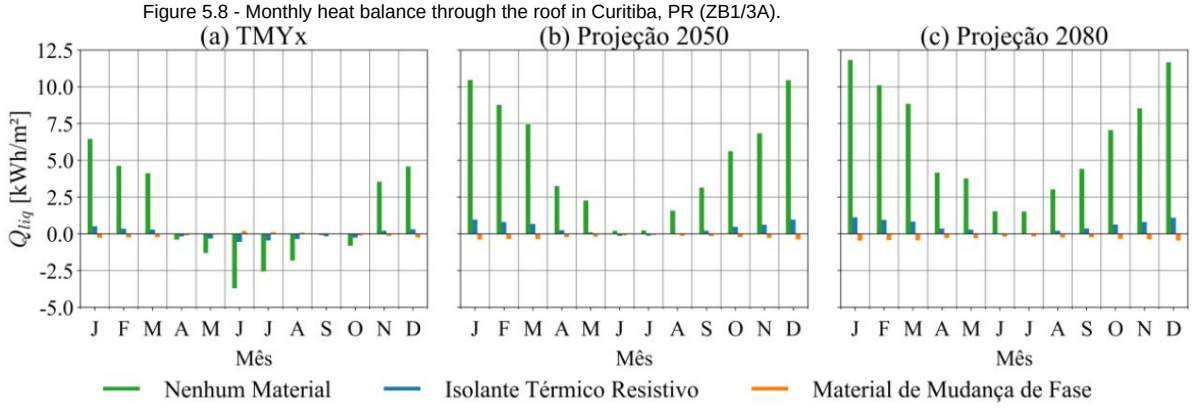

Source: the Author.

In contrast, the absence of any material makes heat transfer across the surface much more sensitive to temperature gradients; comparing the envelope in question with those that have the application of insulating material, it is visible that the *plenum* exchanges heat with the external environment in an intense way, in particular, at the height of summer and winter: for the typical year, as the envelopes with PCM and insulation present, respectively, annual heat gains of 2.12 kWh/m² and 4.57 kWh/m² and

annual heat losses of -3.07 kWh/m² and -5.11 kWh/m², the roof without any material applied records annual gains of 47.53 kWh/m² and losses of -34.82 kWh/m².

Between May and August of the TMY, the building without material on the roof records the highest heat losses, with a minimum of -3.68 kWh/m² in June, and the highest EUI values with the HVAC system. The low temperature of the return air in the *plenum,* which, when mixed with the external air, demands more thermal energy from the heating coils to reach the *setpoint;* in certain months of autumn (April and May) and spring (September and October), for the climate represented by the TMYx file, and also June and July of the climate projection for 2050, present heat balances close to zero, justifying by thermal balance between the surface faces, depending on external temperatures, solar radiation and return air temperature in the *plenum.* The large heat gains in the summer period stand out for both climate projections, which exceed 5 kWh/m².

Figure 5.9 - Hourly curves of operating temperature in the *plenum* and heat flow by conduction on the internal surface of the roof during a typical winter week in Curitiba, PR (ZB1/3A).

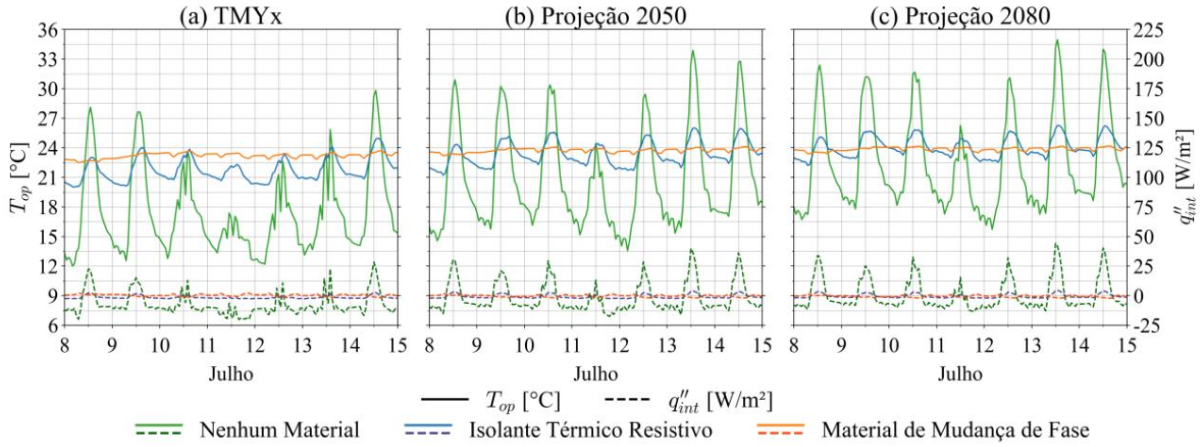

Source: the Author.

Figure 5.10 - Hourly behavior of the physical state of the PCM applied to the roof during a typical winter week in Curitiba, PR (ZB1/3A).

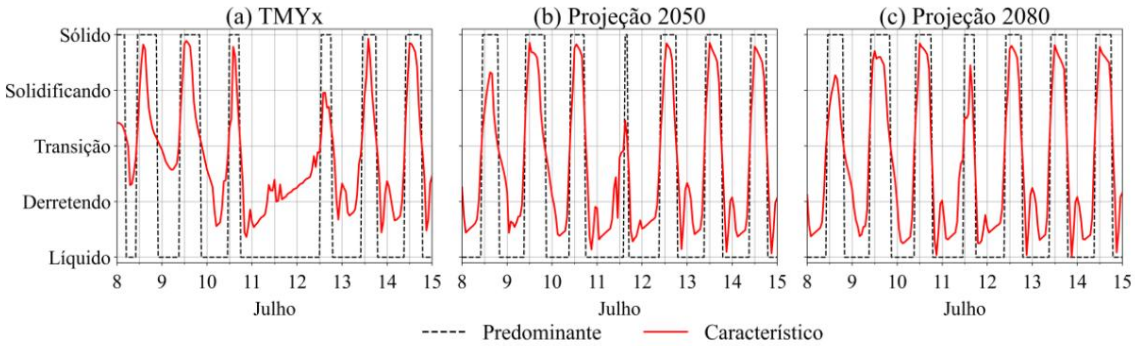

Source: the Author.

From Figure 5.9, it can be seen that the PCM envelope is capable of maintaining the operating temperature of the space almost constant throughout the evaluated week, for all simulated climates, keeping the average temperature during occupied hours below 24°C. Even during the typical winter week, the envelope without insulating material causes high operating temperatures and large thermal amplitudes, with variations of almost 17°C daily; the heat fluxes through the roof throughout the week, in this application, reinforce this behavior of the gradients.

The characteristic physical state of the PCM on the roof – Figure 5.10 – shows phase change cycles with greater definition compared to the behavior of the material on the south facade, but less clear than on the north facade. The thickness of the material, 17 cm, prevents its entire volume from changing phase in a uniform manner, whose hysteresis cycles are incomplete and a kind of stratification of the physical state

it is visible; the behavior of the characteristic physical state varies within the phase transition region and with a tendency to solidification, especially for the simulation with the TMYx file. In this climatic situation, the volume of material mostly does not reach the liquid state.

5.2 Results for bioclimatic zone 8/1A (Rio de Janeiro, RJ)

Naturally, the typology studied, in the climate of bioclimatic zone 8, presents higher monthly EUI values when compared to other climatic regions (see Figure 5.11).

Figure 5.11 - Monthly Energy Use Intensity with HVAC systems in Rio de Janeiro, RJ (ZB8/1A).

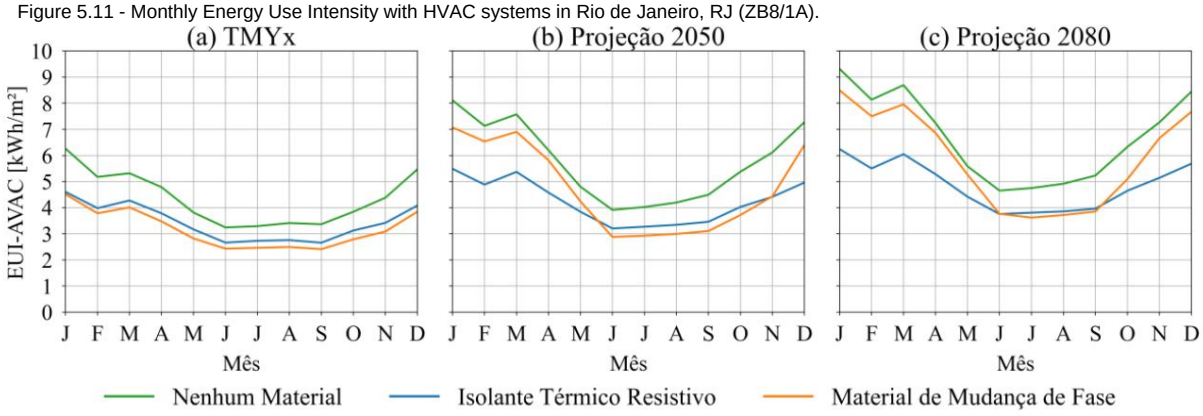

Source: the Author.

However, in climate projections, the EUI of the building with phase change material is close to the EUI of the simulated building without any insulating material, being, annually, around 12.1% (2050) and 20.7% (2080) higher that the envelope with resistive thermal insulation, highlighting the months of January to May and November and December; during the winter and spring period, projected for 2050 (Figure 5.11 (b)), the PCM results in the lowest values of energy consumed, which only happens during winter for the 2080 projection, visible in Figure 5.11 (c); the envelope with resistive thermal insulation presents annual EUI reductions of 21.2%, 26.5% and 27.5% for the simulated climates, respectively, compared to the building without insulating material.

5.2.1 North facade (thermal zone 3)

Observing Figure 5.12, the absence of insulating material again causes high monthly heat gains throughout the year, resulting annually in 95.01 kWh/m², 131.11 kWh/m² and 143.19 kWh/m² for respective simulated climates.

Figure 5.12 - Monthly heat balance across the north facade in Rio de Janeiro, RJ (ZB8/1A).

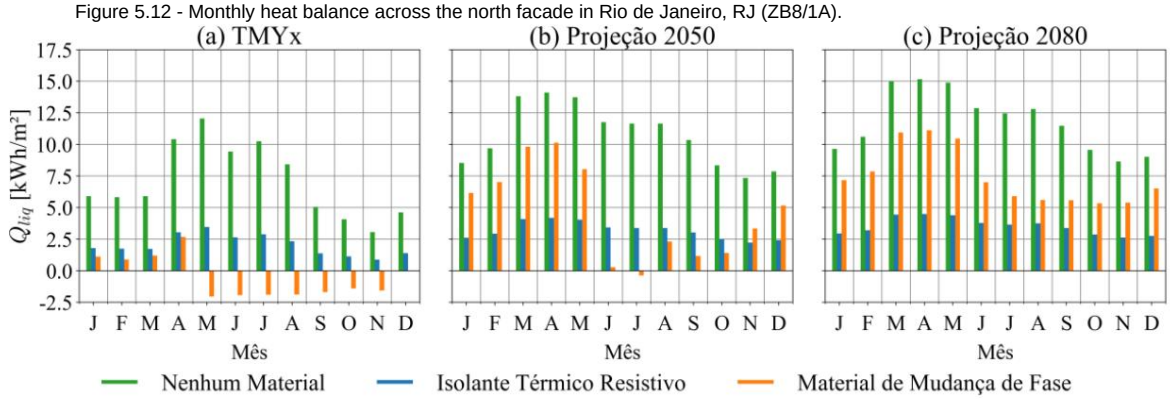

Source: the Author.

The phase change material produces monthly heat losses between May and November of the TMY, shown in Figure 5.12 (a), the period in which the greatest difference in monthly EUI occurs for this application compared to the others. The insulating material can maintain a uniform and similar profile – with differences in

magnitude – among all climate behaviors. For climate projections, heat gains through the north facade with PCM exceed those of the same facade with resistive thermal insulation: for the 2050 projection they are 57.86%, while for the climate projected for 2080 they reach 113.75% more.

The typical week defined for Rio de Janeiro, according to the TMYx file, is from December 24th to 31st, presenting an average close to the annual average; Since the city's climate does not show large differences in temperature throughout the seasons, the file does not specify a typical seasonal week. Visibly through Figure 5.13 (b) and (c), the average radiant temperatures and heat fluxes through the facade with PCM are higher than the results for the resistive thermal insulator – the average radiant temperatures are around 0.3°C higher – validating the high consumption in this case during the month of December for climate projections, a behavior opposite to that presented for the same envelope in the typical meteorological year; for the simulated climate, the average radiant temperature for the case with insulation is about 0.4°C higher than for the case with PCM.

Figure 5.13 - Hourly curves of average radiant temperature in thermal zone 3 and heat flow by conduction on the internal face of the north facade during a typical week in Rio de Janeiro, RJ (ZB8/1A).

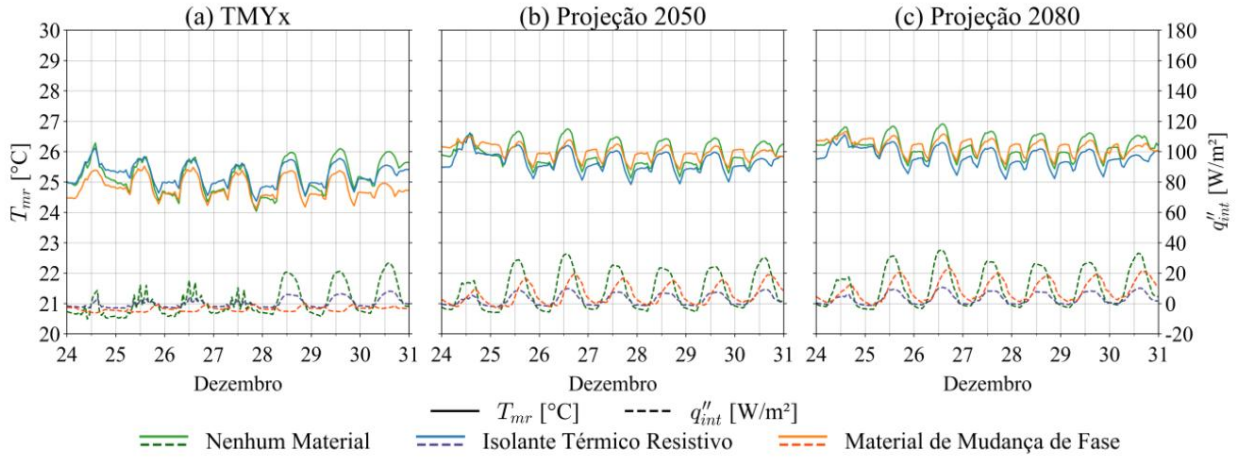

Source: the Author.

The characteristic physical state of the phase change material, evaluated for the typical week, in the climate projections of 2050 (Figure 5.14 (a)) and 2080 (Figure 5.14 (b)) show a constantly liquid physical state, justifying the high use of energy of the month in question and in the other summer months and the heat flow and temperature behaviors expressed in Figure 5.13.

Figure 5.14 - Hourly behavior of the physical state of the PCM applied to the north façade during a typical week in Rio de Janeiro, RJ (ZB8/1A).

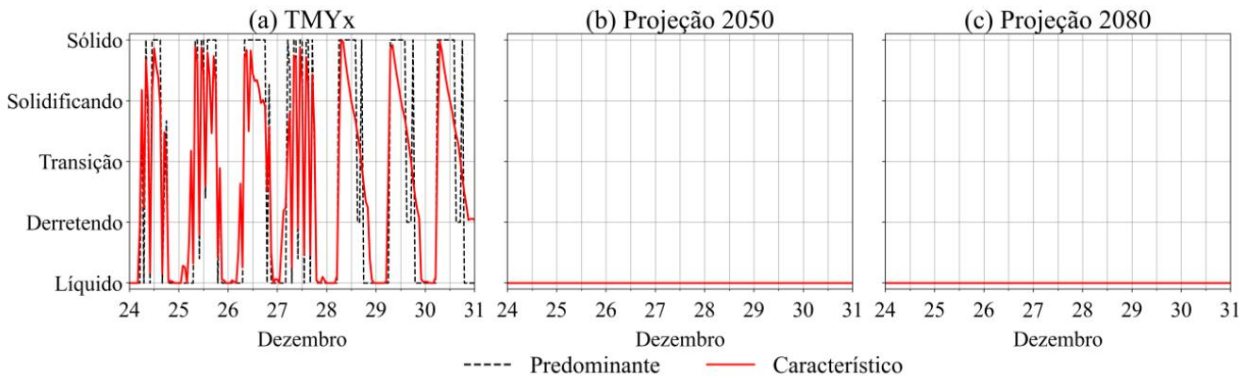

Source: the Author.

Given the high temperatures, even during the typical meteorological year, the high frequency of physical state changes during the day can be observed especially between the 27th and 28th. Possibly, a proximity between internal and external temperatures occurs, which also reduces

the heat flow by conduction within the surface; This temperature trend maintains a significant volume of the PCM in a transitional physical state, subject to state variations more easily.

5.2.2 Thermal zone with south facade (Zone 1)

The behavior of the monthly heat balance for the south façade resembles the monthly energy consumption illustrated in Figure 5.15, especially when observing the envelope with phase change material: as the monthly heat balance denotes loss of thermal energy, the The monthly EUI value for the respective building becomes the lowest among the three simulated envelopes, with emphasis on projections of future climates. The Pearson correlation coefficients, for the 2050 and 2080 climate projections, are 0.940 and 0.973, respectively, denoting a very strong correlation between the variables.

Figure 5.15 - Monthly heat balance through the south facade in Rio de Janeiro, RJ (ZB8/1A).

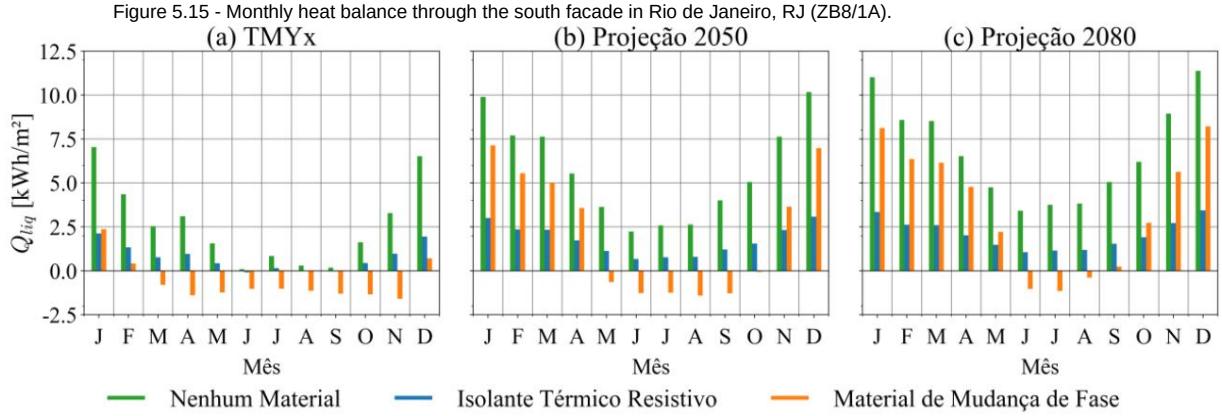

Source: the Author.

Similar to thermal zone 3, thermal zone 1, observing Figure 5.16, presents higher average radiant temperature results on the facade with phase change material than those presented by the wall with resistive thermal insulation in climate projections. The weekly average for this application is 26.09 and 26.26°C for the climates of 2050 and 2080; in the case of the insulating envelope, the average in these periods reduces to 25.78 and 25.90°C.

Figure 5.16 - Hourly curves of average radiant temperature in thermal zone 1 and heat flow by conduction on the internal face of the south facade during a typical week in Rio de Janeiro, RJ (ZB8/1A).

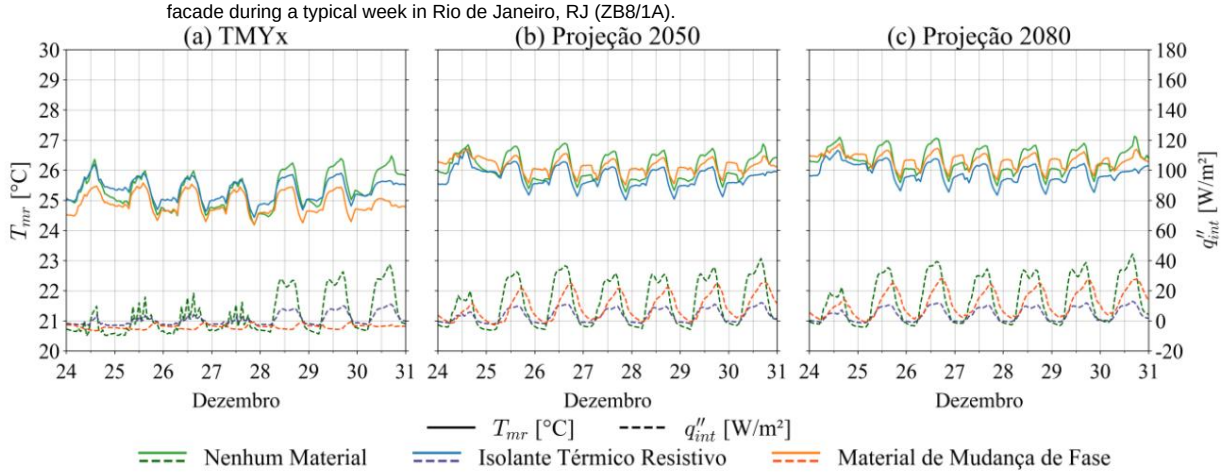

Source: the Author.

According to Figures Figure 5.11 and Figure 5.15 (b) and (c), in December of the projected climates, the energy consumption and heat balance for the envelope with phase change material present superior results compared to the values for the envelope with resistive thermal insulator; although the absence of direct solar irradiation on this surface, the high external temperatures and the low thickness of the

4 cm material, compared to other applications, the PCM is in a liquid state throughout the week of December (Figure 5.17 (b) and (c)), increasing the thermal transmittance of the surface.

Figure 5.17 - Hourly behavior of the physical state of the PCM applied to the south facade during a typical week in Rio de Janeiro, RJ (ZB8/1A).

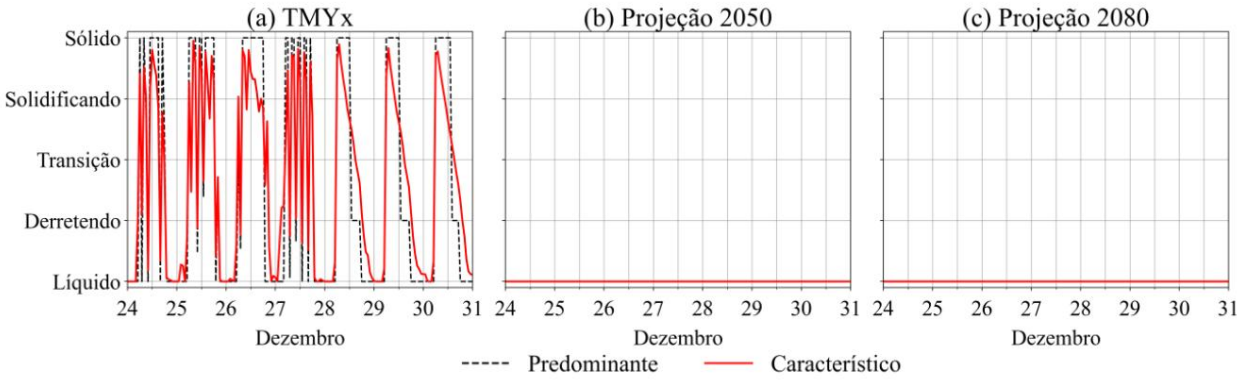

Source: the Author.

5.2.3 Coverage *(plenum)*

Similar to other surfaces, the monthly heat balance across the surface corroborates the behavior of monthly energy consumption with air conditioning – see Figure 5.18. The cover without insulating material allows significant heat gains to the return *plenum* in all months of the year, with values considerably higher than those presented by other envelope constructions; for this coverage composition, Pearson correlation coefficients between the monthly heat balance and the monthly EUI are obtained as 0.920 (TMYx), 0.964 (2050) and 0.963 (2080), demonstrating a strong correlation between the metrics.

Figure 5.18 - Monthly heat balance through the roof in Rio de Janeiro, RJ (ZB8/1A).

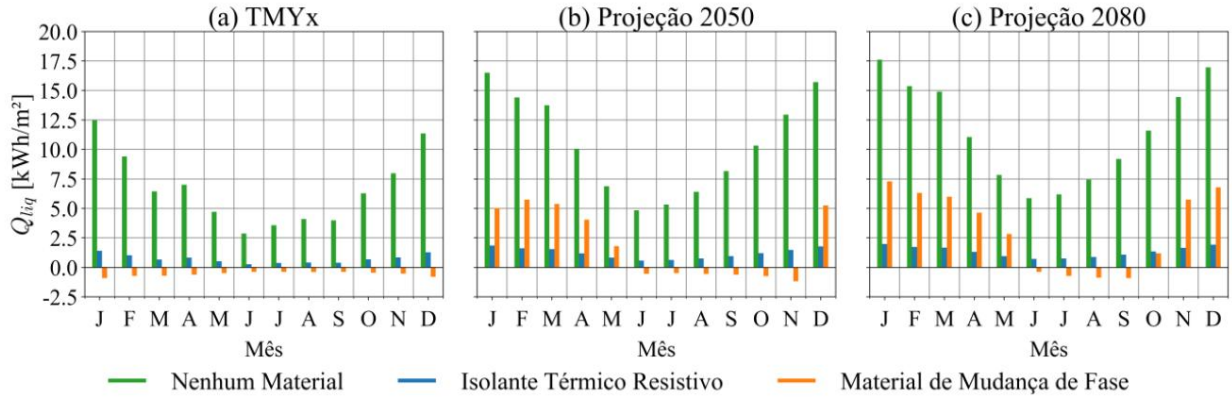

Source: the Author.

The PCM leads to significant heat gains in simulations with future climates compared to those presented in the roof with resistive thermal insulation, however, it is capable of generating negative monthly heat balances in the winter and spring months, coinciding with periods of minimum EUI of the envelope ; The resistive thermal insulator is capable of significantly reducing heat flow in all climates, resulting in less significant heat gains than other applications.

Corroborating the analyzes of the north and south facades, more significantly, the operating temperature of the upper *plenum* is observed in the case of the roof with PCM when compared to the structure with resistive thermal insulation in climate projections; the weekly average operating temperature exceeds it by 2°C in 2050 and 2.4°C in the climate projection of 2080. Furthermore, the range of this temperature is also significant, contrasting with the other facades. The thermal insulating roof can, regardless of the simulated climate, maintain low levels of heat flow, which guarantees adequate temperatures in the space, reaching a maximum weekly average in the future climate of 2080, with 26.3°C.

Again, the various heat flux and temperature peaks, explained in Figure 5.19 (a) for the covering without material, can be justified by the temperature balance between the inner face and the surface core; For the typical meteorological year, this cover produces an average operating temperature of 28.7°C, about 3°C above the others.

Figure 5.19 - Hourly curves of operating temperature in the *plenum* and heat flux by conduction on the internal surface of the roof during a typical week in Rio de Janeiro, RJ (ZB8/1A).

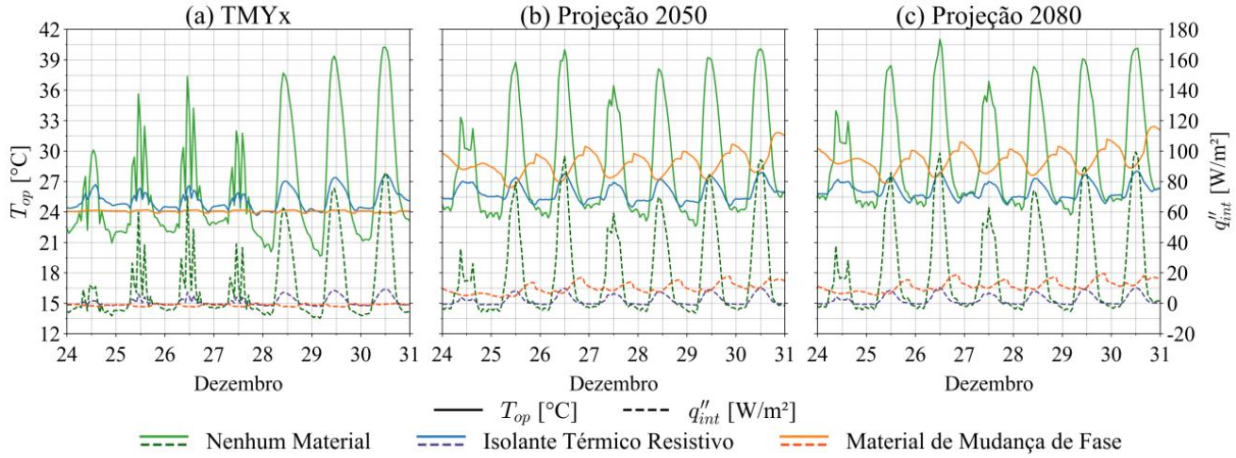

Source: the Author.

Although there are 14 cm of PCM on the roof, the material remains in a liquid state during typical weeks simulated with future climate files, as expressed by the curves in Figure 5.20 (b) and (c). This keeps the *plenum,* more specifically the return air, at high temperatures that are less advantageous for conditioning, which demands more from the HVAC system to remove thermal energy from the mixing air that is blown into the thermal zones.

Figure 5.20 - Hourly behavior of the physical state of the PCM applied to coverage during a typical week in Rio de Janeiro, RJ (ZB8/1A).

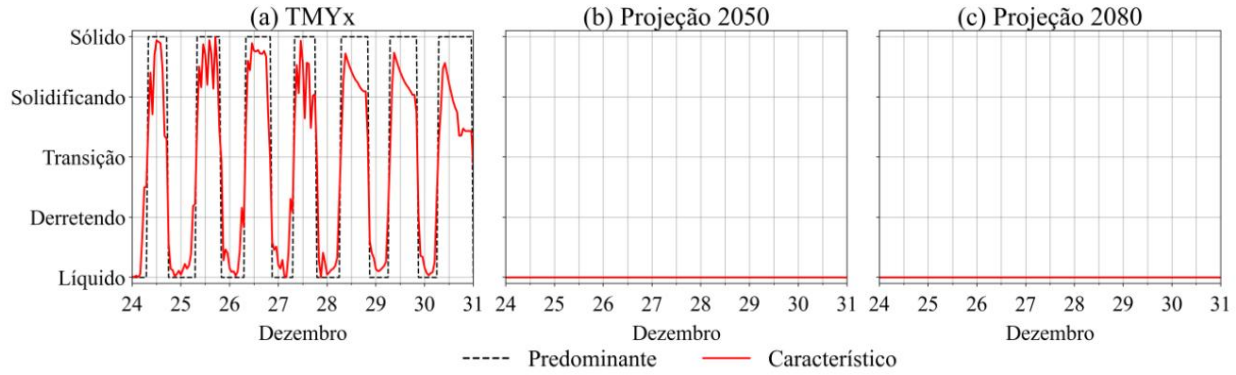

Source: the Author.

6 CONCLUSION

The present work proposed to evaluate the thermal and energetic behavior in future climates of a commercial building due to the implementation of different materials in the envelope and their impacts on the climate adaptability and thermal resilience of this building. Using the *software EnergyPlus* and *Python* codes for analysis and processing of *output data,* three types of envelope were studied: with resistive thermal insulator, according to ASHRAE; with phase change material SP24E, geometrically replacing this insulator; and without any insulating material, having the highest thermal transmittance among the envelopes considered. A prototype thermoenergetic model built and made available by the United States Department of Energy was used, whose systems are in accordance with ASHRAE standards; two cities representing areas were selected

bioclimatic criteria defined by ABNT (1 and 8), coinciding with those of the American association (3A and 1A), for carrying out simulations under different climatic behaviors.

Projections of future climate change, for the representative years of 2050 and 2080, were incorporated into the climate files, necessary for thermoenergetic simulations, through the statistical morphing downscaling methodology using the CCWorldWeatherGen tool and data from the HadCM3 Global Atmospheric *Circulation Model ,* made available by the Intergovernmental Panel on Climate Change (IPCC), for the A2, medium-high emissions scenario. The building metrics consisted of the monthly Energy Use Intensity (EUI) for air conditioning of the environments and the behavior of the monthly heat balances through the envelopes; at the scale of thermal zones, hourly profiles were studied in typical weeks of the average radiant temperature, operating temperature and heat flux on the internal face of the facade surfaces, and also the hourly characteristic physical state of the PCM on the respective surfaces where the material was applied.

From the results obtained and respective analyses, it appears that the work achieves the proposed objectives and, therefore, it is concluded that:

- The implementation of the phase change material with operating temperatures within the *setpoint* range of the air conditioning system results in better thermal and energy performance of the building in regions with mild climates compared to the use of resistive thermal insulators, presenting lower EUI values ; however, in places where climate projections indicate a significant increase in temperatures, the application of PCM may be unfeasible because heat transfer through the surface intensifies while the material remains in a liquid state during the building's operation. In this scenario, insulating materials prove to be more beneficial from the point of view of energy efficiency than PCM;

- The simultaneous combination of passive applications (in the thermal zone envelope) and active (in the *plenum envelope)* enhances the impact of implementing the phase change material throughout the external envelope, maintaining adequate levels of average radiant temperature and operating temperature depending on to the HVAC system *setpoints ;*
- Climate change appears to be an important aspect for the evaluation and design of envelopes and its consideration in thermoenergetic simulations is a relevant tool for studying the performance of the building during its useful life. The Pearson correlation coefficients calculated make it clear that, with increasing temperatures, heat gains through the envelope, particularly in a building with poor thermal insulation, will dictate energy consumption with air conditioning, which denotes the imperative of implementing
  envelope strategies to ensure adaptability and climate resilience of buildings;
- Being a naturally passive and climate-sensitive application, the definition of the PCM operating temperature range must be designed primarily by observing local meteorological conditions, concomitantly with the definition of thermodynamic parameters; • The increase in
  the thermal conductivity of the phase change material, although it brings benefits from the point of view of the thermal hysteresis cycle, can negatively impact the performance of the envelope where the material is applied, since the PCM can remain in a single physical state , thus losing the latent heat storage capacity and increasing the thermal transmittance of the surface where it is applied, intensifying heat gains.

For future work, it is suggested to include the economic evaluation of the envelopes, consideration of different climatic zones and the application of conventional materials from national civil construction as a reference, which already have relevant thermal mass. PCMs work based on hysteresis cycles and, depending on the number of cycles, the material may present variations in its thermal properties.
In this sense, the periodic replacement of the phase change material plays a relevant role, such as, for example, adapting the transmittance of the envelope to increasing temperatures or combining the materials into a composite surface. Other suggestions involve the consideration of different HVAC typologies and systems, in order to study the passive and active effects of PCM implementation and the impact on partial load performance of air conditioning equipment. Furthermore, the
Envelope characteristics can be parameterized in subsequent work, with the objective of optimizing energy efficiency, thermal comfort and construction and operating costs of the building.

BIBLIOGRAPHIC REFERENCES

AKEIBER, Hussein; NEJAT, Payam; MAJID, Muhd Zaimi Abd.; WAHID, Mazlan A.; JOMEHZADEH, Fatemeh; FAMILEH, Iman Zeynali; CALAUTIT, John Kaiser; HUGHES, Ben Richard; ZAKI, Sheikh Ahmad. A review on phase change material (PCM) for sustainable passive cooling in building envelopes. **Renewable And Sustainable Energy Reviews,** [SL], v. 60, p. 1470-1497, jul. 2016. Elsevier BV. http://dx.doi.org/10.1016/j.rser.2016.03.036.

AL-JANABI, Ali; KAVGIC, Miroslava. **Application and sensitivity analysis of the phase change material hysteresis method in EnergyPlus: A case study.** Applied Thermal Engineering, [SL], v. 162, p.1-19, nov. 2019. Elsevier BV. http://dx.doi.org/10.1016/j.applthermaleng.2019.114222.

AL-YASIRI, Qudama; SZABÓ, Márta. Incorporation of phase change materials into building envelope for thermal comfort and energy saving: a comprehensive analysis. **Journal Of Building Engineering,** [SL], v. 36, p. 102122, apr. 2021. Elsevier BV. http://dx.doi.org/10.1016/j.jobe.2020.102122.

ASHRAE. **ANSI/ASHRAE/IES Standard 90.1-2019 – Energy Standard for Buildings Except Low Rise Residential Buildings.** American Society of Heating, Refrigerating and Airconditioning Engineers, 2019.

BRAZILIAN ASSOCIATION OF TECHNICAL STANDARDS - **ABNT. NBR 15220-3:** Thermal Performance of Buildings - Part 3: Brazilian bioclimatic zoning and construction guidelines for single-family homes of social interest. Rio de Janeiro: ABNT, 2005.

BAGLIVO, Cristina; CONGEDO, Paolo Maria; MURRONE, Graziano; LEZZI, Delilah. Long-term predictive energy analysis of a high-performance building in a Mediterranean climate under climate change. **Energy,** [SL], 2022. v. 238, P. 121641, Jan. Elsevier BV. http://dx.doi.org/10.1016/j.energy.2021.121641.

BELCHER, If; HACKER, Jn; POWELL, Ds. Constructing design weather data for future climates. **Building Services Engineering Research And Technology,** [SL], v. 26, no. 1, p. 49-61, Feb. 2005. SAGE Publications. http://dx.doi.org/10.1191/0143624405bt112oa.

BERGMAN, Theodore L.; LAVINE, Adrienne S.; INCROPERA, Frank P.; DEWITT, David P. **Fundamentals of Heat and Mass Transfer.** 7. ed. Rio de Janeiro: Ltc, 2013. 1699 p.

CARLUCCI, Francesco; CANNAVALE, Alessandro; TRIGGIANO, Angela Alessia; SQUICCIARINI, Amalia; FIORITO, Francesco. Phase Change Material Integration in Building Envelopes in Different Building Types and Climates: modeling the benefits of active and passive strategies. **Applied Sciences,** [SL], v. 11, no. 10, p. 4680, May 20, 2021. MDPI AG. http://dx.doi.org/10.3390/app11104680.

CRAWLEY, Drury; LAWRIE, Linda. Rethinking the TMY: is the “typical” meteorological year best for building performance simulation?. **Building Simulation Conference Proceedings,** [SL], v. 14, no. 1, p. 1-8, 7 Dec. 2015. IBPSA. http://dx.doi.org/10.26868/25222708.2015.2707.

D'AGOSTINO, D.; PARKER, D.; EPIFANI, I.; CRAWLEY, D.; LAWRIE, L.. How will future climate impact the design and performance of nearly zero energy buildings (NZEBs)? **Energy,** [SL], v. 240, p. 122479, Feb. 2022. Elsevier BV. http://dx.doi.org/10.1016/j.energy.2021.122479.

DONATE. **EnergyPlus Engineering Reference.** US Department of Energy, 2019.

DONATE. **EnergyPlus.** Version 9.2. US Department of Energy, https://energyplus.net/. Accessed on: 02 Jul. 2022a.

DONATE. **Prototype Building Models.** US Department of Energy. Available at: https://www.energycodes.gov/prototype-building-models. Accessed on: 10 Nov. 2022b.

DONATE. **Types of Insulation.** US Department of Energy. Available in: https://www.energy.gov/energysaver/types insulation#:~:text=The%20most%20common%20types%20of%20materials%20used%20for%20loose%2Dfill,(rock%20or%20slag)%20wool. Accessed on: 10 Dec. 2022c.

Energy research company. Ministry of Mines and Energy. **Atlas of Energy Efficiency Brazil 2021.** [SI]: EPE, 2022. Available at: https://www.epe.gov.br/pt/publicacoes-dados Abertos/publicacoes/atlas-da-eficiencia-energetica-brasil-2021 . Accessed on: 16 Feb. 2023.

FANG, Zhaosong; LI, Nan; LI, Baizhan; LUO, Guozhi; HUANG, Yanqi. The effect of building envelope insulation on cooling energy consumption in summer. **Energy And Buildings,** [SL], v. 77, p. 197-205, Jul. 2014. Elsevier BV. http://dx.doi.org/10.1016/j.enbuild.2014.03.030.

FILIPPINI, Lorenzo Olivo; SARTORI, Gabriela; TORRES, Maurício Carvalho Ayres. The impact of PCM applications on thermal comfort in standardized preschool designs in 2 Brazilian climatic zones. **Building Simulation Conference Proceedings,** [SL], v. 17, no. 1, p. 2749-2756, 1 September. 2021. KU Leuven. http://dx.doi.org/10.26868/25222708.2021.30855.

GRANDERSON, Jessica; LIN, Guanjing; HARDING, Ari; IM, Piljae; CHEN, Yan. Building fault detection data to aid diagnostic algorithm creation and performance testing. **Scientific Data,** [SL], v. 7, no. 1, p. 1-15, 24 Feb. 2020. Springer Science and Business Media LLC. http://dx.doi.org/10.1038/s41597-020-0398-6.

IEA. International Energy Agency. **Building Envelope.** Available in: https://www.iea.org/reports/building-envelopes. Accessed on: 26 Nov. 2022a.

IEA. International Energy Agency. **Buildings.** Available at: https://www.iea.org/topics/buildings. Accessed on: 15 Aug. 2022b.

IEA. International Energy Agency. **Cooling.** Available at: https://www.iea.org/fuels-and technologies/cooling. Accessed on: 15 Aug. 2022c.

IEA. International Energy Agency. **The Future of Cooling:** opportunities for energy-efficient air conditioning. 2018. Available at: https://www.iea.org/reports/the-future-of-cooling. Accessed on: 15 Aug. 2022d.

BRAZILIAN INSTITUTE OF GEOGRAPHY AND STATISTICS. **The country's estimated population reaches 213.3 in millions in 2021.** **population in 2021.** Available in: https://agenciadenoticias.ibge.gov.br/agencia-noticias/2012-agencia-de-noticias/noticias/31458-estimated-population-of-the-country-reaches-213-3-million-inhabitants-in 2021#:~:text=O%20munic%C3%ADpio%20de%20S%C3%A3o%20Paulo,(2%2C7%20milh%C3%B5es) . Accessed on: 28 Nov. 2022.

IPCC. Intergovernmental Panel On Climate Change. **HadCM3 Climate Scenario Data.** Data Distribution Center. Available at: https://www.ipcc-data.org/sim/gcm_clim/SRES_TAR/hadcm3_download.html. Accessed on: 28 Nov. 2022.

JENTSCH, Mark F.; JAMES, Patrick AB; BOURIKAS, Leonidas; BAHAJ, Abubakr S.. Transforming existing weather data for worldwide locations to enable energy and building performance simulation under future climates. **Renewable Energy,** [SL], v. 55, p. 514-524, jul. 2013. Elsevier BV. http://dx.doi.org/10.1016/j.renene.2012.12.049.

KALBASI, Rasool; AFRAND, Masoud. Which one is more effective to add to building envelope: phase change material, thermal insulation, or their combination to meet zero-carbon-ready buildings?. **Journal Of Cleaner Production,** [SL], v. 367, p. 133032, Sep. 2022. Elsevier BV. http://dx.doi.org/10.1016/j.jclepro.2022.133032.

KALBASI, Rasool; HASSANI, Parsa. Buildings with less HVAC power demand by incorporating PCM into envelopes taking into account ASHRAE climate classification. **Journal Of Building Engineering,** [SL], v. 51, p. 104303, Jul. 2022. Elsevier BV. http://dx.doi.org/10.1016/j.jobe.2022.104303.

LIU, Zhengxuan; YU, Zhun (Jerry); YANG, Tingting; QIN, Di; LI, Shuisheng; ZHANG, Guoqiang; HAGHIGHAT, Fariborz; JOYBARI, Mahmood Mastani. A review on macro-encapsulated phase change material for building envelope applications. **Building And Environment,** [SL], v. 144, p. 281-294, Oct. 2018. Elsevier BV. http://dx.doi.org/10.1016/j.buildenv.2018.08.030.

MELO, Ana Paula; LAMBERTS, Roberto; VERSAGE, Rogério de Souza; ZHANG, Yi. Is Thermal Insulation Always Beneficial in Hot Climates? **Building Simulation Conference Proceedings,** [SL], v. 14, no. 1, p. 1353-1360, 7 Dec. 2015. IBPSA. http://dx.doi.org/10.26868/25222708.2015.2188.

PAROUTOGLOU, Evdoxia et al. A PCM based cooling system for office buildings: a state-of-the-art review. **E3s Web Of Conferences,** [SL], 111, p.1-8, 2019. EDP Sciences. http://dx.doi.org/10.1051/e3sconf/201911101026.

PBE Edifica. **INMET 2018 climatic archives.** 2020. Available at: http://pbeedifica.com.br/arquivos climaticos/inmet2018. Accessed on: 10 Jan. 2023.

POPESCU, C. -M.. Wood as bio-based building material. **Performance Of Bio-Based Building Materials,** [SL], p. 21-96, 2017. Elsevier. http://dx.doi.org/10.1016/b978-0-08-100982-6.00002-1.

RATHORE, Pushpendra Kumar Singh; GUPTA, Naveen Kumar; YADAV, Devanand; SHUKLA, Shailendra Kumar; KAUL, Sanjay. Thermal performance of the building envelope integrated with phase change material for thermal energy storage: an updated review. **Sustainable Cities And Society,** [SL], v. 79, p. 103690, apr. 2022. Elsevier BV. http://dx.doi.org/10.1016/j.scs.2022.103690.

UK. Hadley Center. Met Office. **HadCM3: Met Office climate prediction model.** Available in: https://www.metoffice.gov.uk/research/approach/modelling-systems/unified-model/climate models/hadcm3. Accessed on: 01 Dec. 2022.

RODRIGUES, Eugénio; FERNANDES, Marco S.. Overheating risk in Mediterranean residential buildings: comparison of current and future climate scenarios. **Applied Energy,** [SL], v. 259, p. 114110, Feb. 2020. Elsevier BV. http://dx.doi.org/10.1016/j.apenergy.2019.114110.

RUBITHERM. **BUILDINGS.** 2022. Available at: https://www.rubitherm.eu/en/applications/building. Accessed on: 18 September. 2022a.

RUBITHERM. **Data Sheet SP24E.** 2022. Available in: https://www.rubitherm.eu/media/products/datasheets/Techdata_,SP24E_EN_12072022.PDF. Accessed 18 Sep. 2022b.

SCHELLER, C., Melo, AP, SORGATO, M., LAMBERTS, R. “Analysis of climate files for simulating the energy performance of buildings”. **Laboratory of Energy Efficiency in Buildings,** Federal University of Santa Catarina. Santa Catarina, 2015.

SURESH, C.; HOTTA, Tapano Kumar; SAHA, Sandip K.. Phase change material incorporation techniques in building envelopes for enhancing the building thermal Comfort-A review. **Energy And Buildings,** [SL], v. 268, p. 112225, Aug. 2022. Elsevier BV. http://dx.doi.org/10.1016/j.enbuild.2022.112225.

TABARES-VELASCO, Paulo Cesar; CHRISTENSEN, Craig; BIANCHI, Marcus. Verification and validation of EnergyPlus phase change material model for opaque wall assemblies. **Building And Environment,** [SL], v. 54, p. 186-196, 2012. Aug. Elsevier BV. http://dx.doi.org/10.1016/j.buildenv.2012.02.019.

UNIVERSITY OF SOUTHAMPTON. **CCWorldWeatherGen.** 2022. Available at: https://energy.soton.ac.uk/ccworldweathergen/. Accessed on: 20 Nov. 2022.

VEERAKUMAR, C.; SREEKUMAR, A.. Phase change material based cold thermal energy storage: Materials, techniques and applications – A review. **International Journal Of Refrigeration,** [sl], v. 67, p.271-289, jul. 2016. Elsevier BV. http://dx.doi.org/10.1016/j.ijrefrig.2015.12.005.

WANG, Xiaonan; LI, Wengui; LUO, Zhiyu; WANG, Kejin; SHAH, Surendra P.. A critical review on phase change materials (PCM) for sustainable and energy efficient buildings: design, characteristics, performance and application. **Energy And Buildings,** [SL], v. 260, p. 111923, apr. 2022. Elsevier BV. http://dx.doi.org/10.1016/j.enbuild.2022.111923.

WMO. World Meteorological Organization. **Updated 30-year reference period reflects changing climate.** 2021. Available at: https://public.wmo.int/en/media/news/updated-30-year-reference-period reflects-changing-climate. Accessed on: 01 Dec. 2022.

YUAN, Feng; YAO, Runming; SADRIZADEH, Sasan; LI, Baiyi; CAO, Guangyu; ZHANG, Shaoxing; ZHOU, Shan; LIU, Hong; BOGDAN, Anna; CROITORU, Cristiana. Thermal comfort in hospital buildings – A literature review. **Journal Of Building Engineering,** [SL], v. 45, p. 103463, Jan. 2022. Elsevier BV. http://dx.doi.org/10.1016/j.jobe.2021.103463.

YÜKSEK, Izzet; KARADAYI, Tülay Tikansak. Energy-Efficient Building Design in the Context of Building Life Cycle. **Energy Efficient Buildings,** [SL], v. 1, no. 5, p. 93-124, 18 Jan. 2017. InTech. http://dx.doi.org/10.5772/66670.

ZASTAWNA-RUMIN, Anna; KISILEWICZ, Tomasz; BERARDI, Umberto. Novel Simulation Algorithm for Modeling the Hysteresis of Phase Change Materials. **Energies,** [SL], v. 13, no. 5, p. 1200, 5 Mar. 2020. MDPI AG. http://dx.doi.org/10.3390/en13051200.

ZILBERBERG, E.; TRAPPER, P.; MEIR, IA; ISAAC, S.. The impact of thermal mass and insulation of building structures on energy efficiency. **Energy And Buildings,** [SL], v. 241, p. 110954, jun. 2021. Elsevier BV. http://dx.doi.org/10.1016/j.enbuild.2021.110954.

APPENDICES

APPENDIX A – Characteristics of solid-liquid type PCM

According to the composition of the solid-liquid type PCM, different characteristics are observed for the macroclassification of the material; in Table AP.1 these characteristics are divided into advantages and disadvantages.

Table AA.1 – Characteristics of solid-liquid PCM.

Type of PCM	Advantages	Disadvantages
Organic	• Availability at different temperatures; • High latent heat of fusion; • Absence of subcooling; • Absence of phase segregation; • Stable after several cycles; • Chemical and physical stability; • Compatibility with capsule materials; • Low corrosivity; • Low environmental impact; • Non-reactive; • Recyclable.	• Low thermal conductivity; • Unstable under high temperatures; • Deformed phase transition; • Some are not compatible with plastic capsules; • Low enthalpy • Different levels of toxicity; • Flammable; • High cost when pure.
Inorganic	• High thermal storage capacity; • Good thermal conductivity; • Easily available; • Low cost; • Low vapor pressure; • Flammable.	• They present superfusion; • Volume variation between phases; • May present phase segregation; • Some are incompatible with metal containers.
Eutectics	• Higher storage density than organic compounds; • Well-defined melting values.	• Costly; • Little thermodynamic data.

Source: adapted from Yasiri and Szabó (2021).

APPENDIX B – Thermal transmittance of the envelope surfaces

Changing the composition of the envelope changes the thermal transmittance value of the surfaces, exceeding the maximum value defined by ASHRAE. Table AB.1 shows the values for the roof and external walls, where “NEM” identifies the envelope without insulating material and “PCM” and the envelope with phase change material; In the case of PCM, a single value is presented between the two physical states since the thermal conductivity does not change (see Appendix D – Phase change material input data for hysteresis simulation), therefore, its thermal resistance is virtually the same.

Table AB.1 – Thermal transmittance of construction surfaces without insulating material.

Climatic zone	[ÿ ^{2}]		[ÿ ^{2}]	
	NOR	PCM	NOR	PCM
1A	5.083	2,098	2.606	2,156
3A	5.083	1,863	2.606	1,839

Source: the Author.

APPENDIX C – Years used to create the TMYx files

Typical meteorological years are constructed by selecting representative months from the reference climate period. Table AC.1 sets out the years from which the months are extracted; In red, years outside the climatic period recommended by the World Meteorological Organization stand out.

Table AC.1 – Years of the climate files used to construct the typical meteorological year.

City	Jan	Feb	Mar	Apr	May	Jun	Jul	Aug	Sep	Oct	Nov	Dec
Curitiba	1977	1987	1977	1964	1993	2008	1980	1965	1986	2017	1977	1990
Rio de Janeiro	1989	1991	2017	1988	1981	1980	1980	1981	2001	1987	2001	1979

Source: the Author.

APPENDIX D – PCM *input* data for hysteresis simulation

Table AD.1 presents the data necessary to simulate the thermal hysteresis of the phase change material in *EnergyPlus.* The data is extracted from the PCM *datasheet* .

Table AD.1 – SP24E material data.

Property	Value	Unit
Melting temperature range Solidification	24-25 (peak at 24)	°C
temperature range Latent heat ( )	23-21 (peak at 22)	°C
	150	kJ/kg
Specific heat ( )	two	kJ/kgK
Specific mass in the solid state	1600	kg/m³
(Specific mass in the liquid state))	1500	kg/m³
(Thermal conductivity ( )	0.5	W/mK

Source: adapted from RubiTherm (2022).

APPENDIX E – Details of the construction of the envelope surfaces

Figure AE.1 illustrates the generic constructions of the roof and facade surfaces external, highlighting the layer of material – insulating or PCM – that is changed between simulations.

Figure AE.1 – Detail of the surface constructions, not to scale.

(a) Roof (b) External Wall

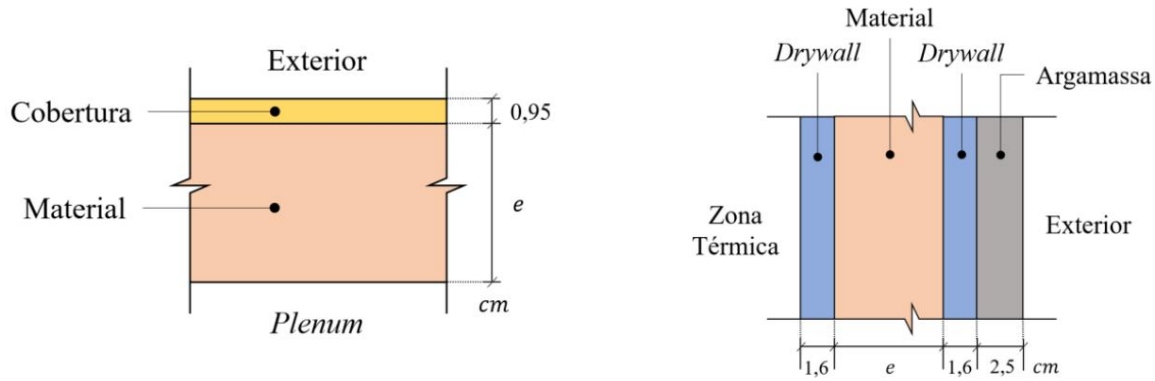

Source: the Author.

APPENDIX F – Climatic behaviors

Figure AF.1 presents the behavior of hourly external dry bulb temperatures (TBS) in each month, according to the climate files used, using *boxplots* to condense temperature information into hourly frequency. This serves as a way of illustrating climate change in relation to the climate of a typical meteorological year. It is also possible to identify

the shift operation , from the morphing technique , being applied to the climate variable in question, by observing uniform displacements between climates.

Figure AF.1 – Behavior of external dry bulb temperatures in simulated climate scenarios.

(a) Curitiba, PR – Bioclimatic Zone 1, ASHRAE 3A

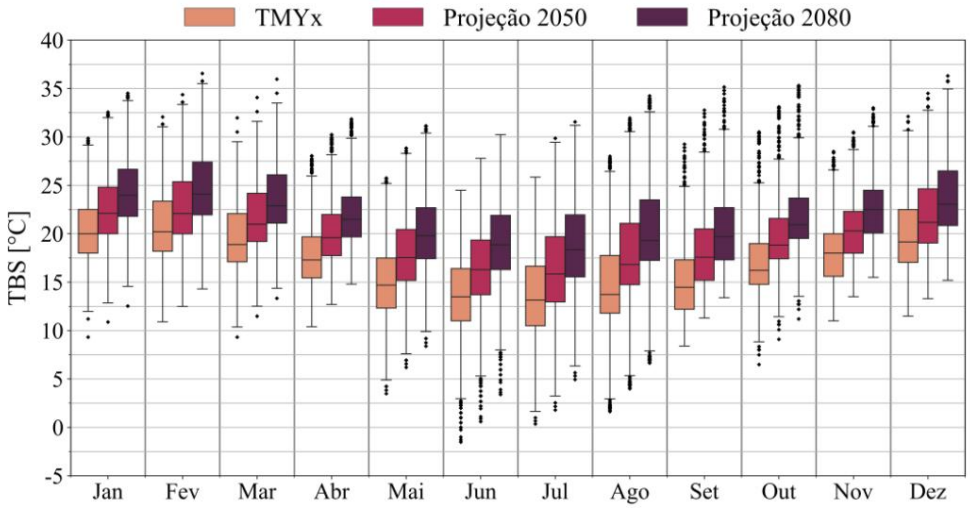

(b) Rio de Janeiro, RJ – Bioclimatic Zone 8, ASHRAE 1A

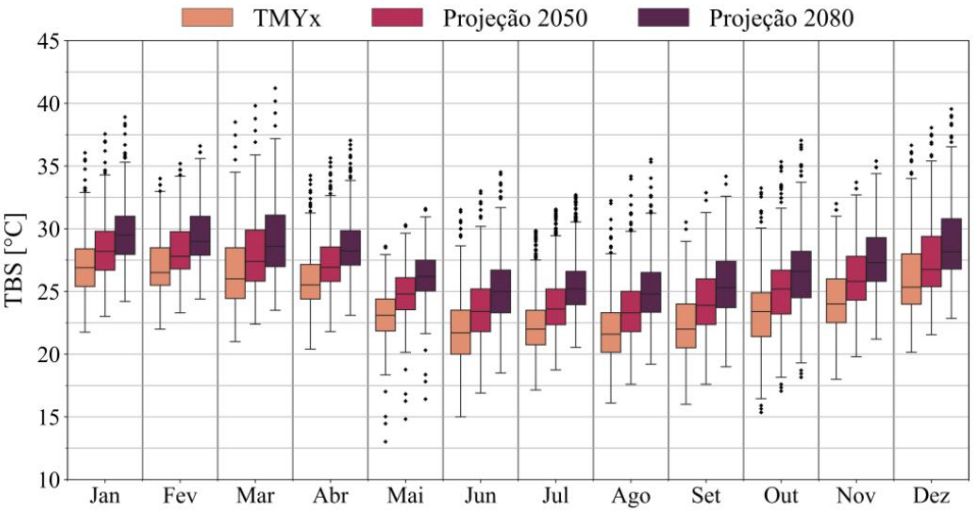

Source: the Author.

Table AF.1 condenses annual information from the three simulated climatic periods: annual average external dry bulb temperature and annual minimums and maximums, in the two simulated bioclimatic zones.
Curitiba records increases of 2.52°C, in the projection for 2050, and 4.65°C in 2080 in the annual average, while the city of Rio de Janeiro, presents less significant increases: 1.59°C in 2050 and 2 .98°C in the projected climate of 2080, compared to the annual average of the typical year.

Table AF.1 – Annual averages and extremes of dry bulb temperatures in the simulated climate scenarios.

Climates	**Curitiba, PR – ZB1 1, ASHRAE 3A Rio de Janeiro, RJ – ZB 8, ASHRAE 1A**
	[°C] í **[°C]** á **[°C]** **[°C]** í **[°C]** á **[°C]**
TMYx	17.17 -1.51 32.10 24.26 13.02 38.51
2050 Projection	19.69 -0.59 34.50 25.86 14.82 39.81
2080 Projection	21.83 -3.39 36.56 27.25 16.42 41.21

Source: the Author.

APPENDIX G – Pearson correlation coefficients

Table AG.1 shows the Pearson correlation coefficient values between the intensity of monthly energy use and the heat balance across the envelope surfaces evaluated.

Table AG.1 – Pearson Correlation Coefficients between monthly EUI and envelope heat balance.

Monthly EUI x heat balance across the north façade						
Climate	**Curitiba, PR (ZB1/3A)**			**Rio de Janeiro, RJ (ZB8/1A)**		
	NEITHER	**ISO PCM**	**ISO PCM**			
TMYx	-0.112	0.597	-0.763	-0.282	0.794	
2050 Projection	-0.134	0.271	-0.121	-0.125	0.815	
2080 projection	-0.282	0.085	0.353	-0.135	0.443	
Monthly EUI x heat balance across the south façade						
Climate	**Curitiba, PR (ZB1/3A)**			**Rio de Janeiro, RJ (ZB8/1A)**		
	NO ISO PCM			**NOR**	**ISO PCM**	
TMYx	-0.144	0.885	0.953	0.918	0.922	0.906
2050 Projection		0.960	-0.957	0.949		0.940
2080 projection		0.956	-0.954	0.944		0.973
Monthly EUI x heat balance across the roof						
Climate	**Curitiba, PR (ZB1/3A)**			**Rio de Janeiro, RJ (ZB8/1A)**		
	NOR	**ISO PCM**		**NOR**	**ISO PCM**	
TMYx	-0.150	0.930	-0.941	0.920	0.856	-0.969
2050 Projection	0.945	0.950	-0.984	0.964	0.928	0.923
2080 Projection	0.971	0.950	-0.988	0.963	0.921	0.983

Source: the Author.

ANNEX A – PCM macroencapsulation alternatives for application in buildings

Figure A.1 – Possible alternatives for macroencapsulation of phase change materials.

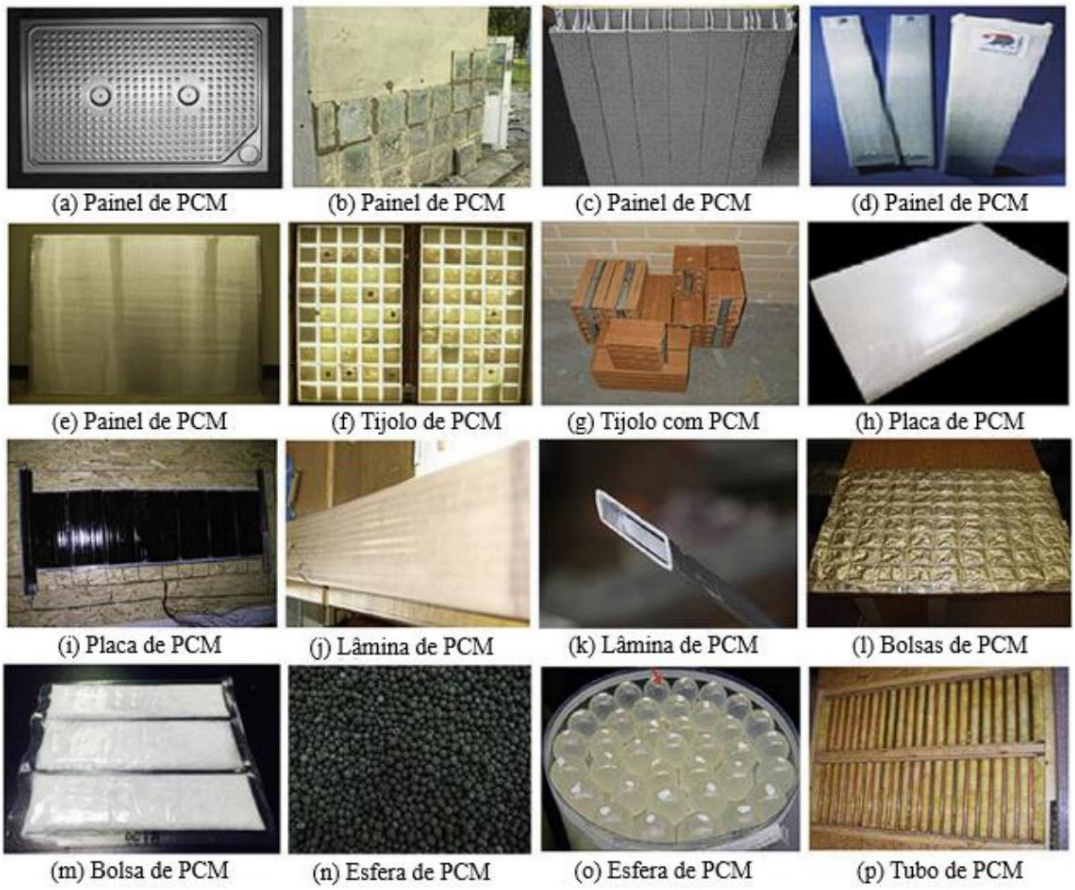

Source: adapted from Liu et al. (2018)

ANNEX B – Schematic diagram of a multi-zone VAV system

Figure B.1 presents a diagram of a single-duct multi-zone VAV system, with *rooftop* unit and economizer cycle, highlighting the return air from the thermal zones to the equipment.

Figure B.1 – Schematic diagram of a single-duct multi-zone VAV system.

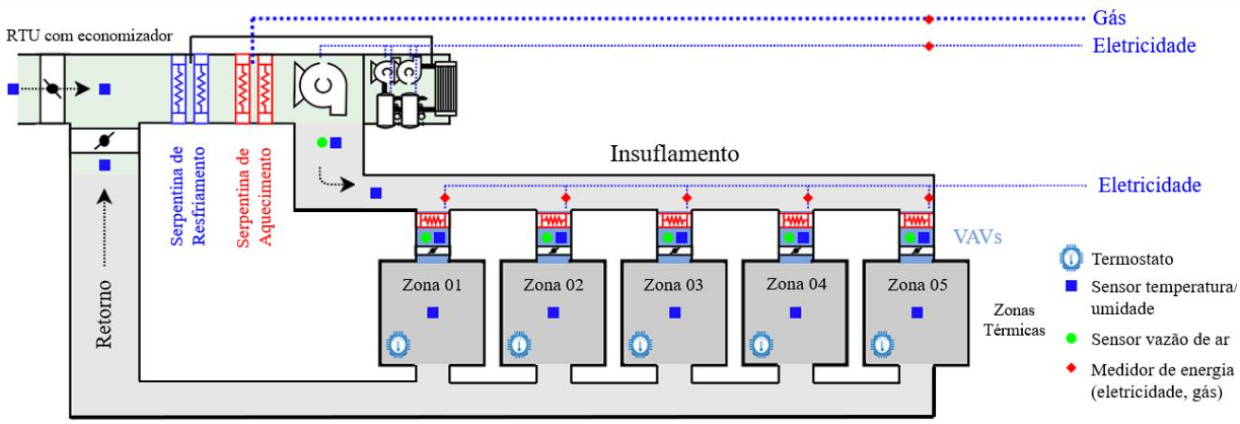

Source: adapted from Granderson et al. (2020).

ANNEX C – PCM SP24E *Datasheet*

Figure C.1 – PCM SP24E *Datasheet* .

The most important data:	Typical Values	
Melting area	**24-25** main peak: 24	[°C]
Congealing area	**23-21** main peak: 22	[°C]
Heat storage capacity ± 7,5% Combination of sensible and latent heat in a temperatur range of 15 °C to 30°C.	**180**	[kJ/kg]
	50	[Wh/kg]*
Specific heat capacity	**2**	[kJ/kg·K]*
Density solid at 15°C	**1,6**	[kg/l]
Density liquid at 35°C	**1,5**	[kg/l]
Volume expansion	**~6**	[%]
Heat conductivity	**~0,5**	[W/(m·K)]
Max. operation temperature	**45**	[°C]
Corrosion	corrosive effect on metals	

The product must be initialized (melt, homogenize and cool to 0 ° C) once before use to achieve the specified properties.
SP-products may absorb release water if stored improperly. This can result in a change of the physical properties given. Storing in closed containers mandatory.

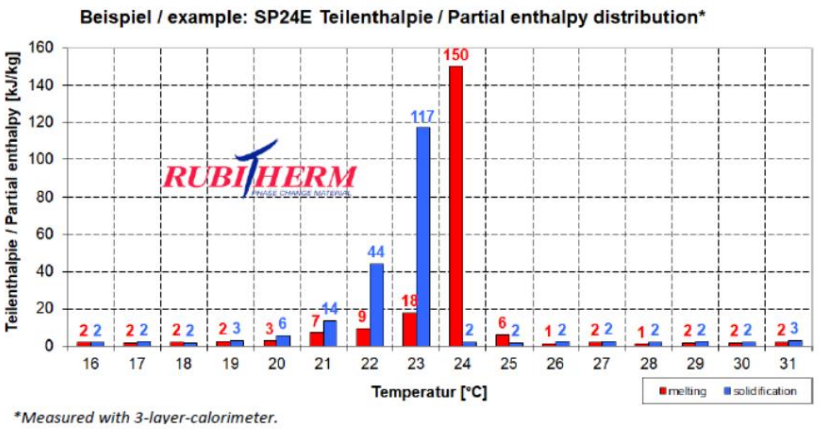

*Measured with 3-layer-calorimeter.

Rubitherm Technologies GmbH
Imhoffweg 6
D-12307 Berlin
phone: +49 (30) 7109622-0
E-Mail: info@rubitherm.com
Web: www.rubitherm.com

The product information given is a non-binding planning aid, subject to technical changes without notice. Version: 12.07.2022

Source: adapted from Rubitherm (2022b).